Hydrocarbon source rock potential and paleoenvironment of lower Miocene diatomites in the Eastern Carpathians Bend Zone (Sibiciu de Sus, Romania)

EMILIA TULAN[1,✉], REINHARD F. SACHSENHOFER[1], GABOR TARI[2], JAKUB WITKOWSKI[3], DAN MIRCEA TĂMAȘ[4], ALEKSANDER HORVAT[5] and ALEXANDRA TĂMAȘ[6]

[1]Montanuniversität Leoben, Peter Tunner Strasse 5, 8700 Leoben, Austria; ✉emilia.tulan@gmail.com, reinhard.sachsenhofer@unileoben.ac.at
[2]OMV Exploration and Production GmbH, Trabrennstrasse 6-8, 1020 Vienna, Austria; gabor.tari@omv.com
[3]Institute of Marine and Environmental Sciences, University of Szczecin, Mickiewicza 18, 70-383 Szczecin, Poland; jakub.witkowski@usz.edu.pl
[4]Department of Geology and Centre for Integrated Geological Studies Babeș-Bolyai University, Kogălniceanu 1, 400084, Cluj-Napoca, Romania; danmircea.tamas@ubbcluj.ro
[5]Institute of Paleontology, Research Centre of the Slovenian Academy of Sciences and Arts Novi trg 2, 1000 Ljubljana, Slovenia; ahorvat@zrc-sazu.si
[6]Department of Earth Sciences, Durham University, DH1 3LE, Durham, United Kingdom; alexandra.tamas@durham.ac.uk

Abstract: Diatomites are prolific hydrocarbon source rocks in many basins worldwide. In the broader Carpathians, diagenetically altered diatomites are called menilites, and menilitic shale successions are regarded as the most prolific hydrocarbon source rocks in the region. The abandoned Sibiciu de Sus quarry, located in the Eastern Carpathian Bend Zone of Romania, provides large exposures of the upper part of the Lower Miocene Upper Menilites, composed of various diatomite lithologies, cherts, menilitic shales and quartz-rich sandstone. The sediments are highly deformed due to soft-sediment deformation and subsequent Miocene to Pliocene contractional tectonics. Twenty-two diatom-bearing samples were examined in order (a) to determine the hydrocarbon source rock potential, (b) to document the diatom assemblages and (c) to interpret the depositional environment. The hydrocarbon potential of the studied rocks is considered good to very good, with an average TOC of 3.77 wt. % (max. 9.57 wt. % TOC) and type II–III kerogen (avg. HI: 384 mg HC/g TOC). Tmax does not exceed 424 °C suggesting that the organic matter is thermally immature. Despite that, the Production Index is high (0.1–0.3), which proves the presence of migrated hydrocarbons. The source potential index (SPI) indicates that the exposed section, if mature, could generate about 1.3 t HC/m². As the diatom preservation does not enable chemical extraction of individual valves, this study describes only genus-level findings. The diatom assemblages are dominated by *Aulacoseira* and *Actinocyclus*, whereas *Ellerbeckia*, *Paralia* and *Rhaphoneis* are rarely observed. The diatom assemblages indicate a nearshore, brackish-water depositional setting.

Keywords: Eastern Carpathian Bend Zone, Miocene, Upper Menilite, diatom assemblages, hydrocarbon source rock.

Introduction

Diatomites are silica-rich sedimentary rocks composed mostly of diatom remains and can be exceptionally prolific hydrocarbon source rocks. Examples include the Miocene Monterey Formation (e.g., Taylor 1976; Mertz 1989) or the Oligocene Pilengskaya Formation and the Middle Miocene Pil'skaya and Kurasiiskaya Formations, which are the best source rocks in Sakhalin (Bazhenova 2002). However, the hydrocarbon potential of diatomites is often overlooked, and one of the aims of this paper is to reduce this knowledge gap in the Carpathian region.

Diagenetically altered diatomaceous rocks in the Carpathians are referred to as menilites (e.g., Krhovsky et al. 1992). It should be pointed out that the term "menilite" refers to a greyish-brown form of the opal mineraloid. The "menilite" is known as *liver opal* or *leberopal* (in German), due to its colour. It is called menilite because it was first described from

Ménilmontant (Paris), France, where it occurs as concretions within bituminous Early Oligocene "Menilite shales" (Lampadius 1809; Knox 1823).

The meaning of menilite in the Carpathians is somewhat different. It stands for a laminated siliceous rock composed of diatom frustules, sponge spicules, radiolaria and fish remains in addition to clay and silt. Although forming only a small part of the entire succession, menilites became eponymous for the fine-grained Oligocene to Lower Miocene succession in the Carpathians, which forms the most important hydrocarbon source rocks in the region (Sachsenhofer et al. 2018a,b and references therein). However, in this paper the menilite rocks will be referred to as menilitic shales (following Soták 2010). The menilitic shales are widespread in the Carpathians and occur both in Lower Oligocene (Lower Menilites) and Lower Miocene (Upper Menilites) strata. In particular, the Lower Menilites are present in the entire Carpathian realm. The extent of the Upper Menilites is more limited, but they include

excellent source rocks in the Ukrainian part of the Eastern Carpathians (Sachsenhofer et al. 2018b; Rauball et al. 2019).

Diatoms appear to have proliferated in the Carpathian realm from the Miocene onwards, as indicated by the widespread occurrence of moderately to well-preserved marine and fresh-water diatoms in Neogene sediments of the Carpathians and their surroundings (e.g., Pantocsek 1886, 1889; Hajós 1968, 1986; Řeháková 1975, 1977; Olshtynska 2001; Ognjanova-Rumenova & Crawford 2012; Ognjanova-Rumenova & Pipík 2015).

In the Eastern Carpathian Bend Zone (ECBZ), an abandoned quarry near Sibiciu de Sus (Buzău county, Romania; Fig. 1) exposes the uppermost part of the Upper Menilites (Lower Miocene) in two mining levels. The uppermost part of the succession at this location is comprised of menilitic shales, quartz-rich sandstone and various diatomite lithologies. The diatomite exposures are several hundred metres long, which makes the Sibiciu de Sus quarry one of the biggest diatomite exposures in the Carpathians. As the exposed rocks are deformed into a NW–SE oriented anticline, the severe deformation and deteriorating outcrop conditions make the correlation of the various lithologies through the quarry somewhat challenging. The main hydrocarbon source rocks within the ECBZ are the menilitic shales, together with organic-rich shales (called dysodiles in Romania, e.g., Paraschiv & Olteanu 1970; Popescu 1995; Dicea 1996). On a side note, the "dysodil" (*stinkkohle* in German) is defined as paper-like lignite, which stinks when it burns (Pierer 1857). Lueger 1904 defined the "dysodil" as paper-like coal composed mainly of bitumen, clay minerals and silica. The meaning of dysodile in Romanian Carpathians refers to paper-like (*șist* in Romanian) bituminous argillaceous and calcareous shale.

Fossil diatoms from Sibiciu de Sus were studied by few authors (e.g., Frunzescu & Brănoiu 2004; Sebe-Rădoi et al. 2017). However, the hydrocarbon potential of the Sibiciu de Sus diatomites has not been studied yet in detail. The main aims of this study were to identify the hydrocarbon potential of the diatomite rocks, to document the fossil diatom assemblage, and to interpret the depositional environment.

Geological setting

The ECBZ is located between the E–W trending Southern and the N–S trending Eastern Carpathians (Fig. 1). The ECBZ is approximately 80 km long and is represented by the external unit of the Carpathian fold-thrust belt (e.g., Săndulescu 1984) comprising, from west to east, the Teleajen, Audia, Macla, Tarcău, Marginal Fold and Subcarpathian Nappes. A brief description of the stratigraphy focused on the Tarcău and Marginal Nappes and partly on the Subcarpathian Nappe is presented below.

The stratigraphy commences with Lower Cretaceous deep marine black shales with some sandy turbidites towards the top (Ștefănescu 1978) followed by Upper Cretaceous variegated shales with radiolarite and calcareous turbidite beds

known as Horgazu and Hangu beds (Schleder et al. 2019). The overlying Paleocene and Eocene successions are represented by the Tarcău Formation, a deep marine sandy sequence and the shale-dominated Colți Formation (Schleder et al. 2019).

The Oligocene to Lower Miocene deposits are characterized by two intercalating lithofacies: the Pucioasa-Fusaru and Bituminous Kliwa facies. The distal "Pucioasa-Fusaru lithofacies" (Pătruț 1955; Grigoraș 1955) represents deep marine shales interbedded with thin mica-rich sandstone beds derived from uplifted nappes in the west (Săndulescu et al., 1981). The more proximal "Bituminous Kliwa lithofacies" (Patrulius et al. 1968; Săndulescu et al. 1995) is located closer to the foreland and, therefore, it has provenance in the East European Platform (e.g., Săndulescu et al. 1995; Grasu et al. 2007).

In the ECBZ, the Bituminous Kliwa lithofacies is divided into several sedimentary units described in detail by Dumitrescu et al. (1970) and their terminology is adopted here. A visual representation of the Bituminous Kliwa lithofacies is provided in Fig. 2.

At the base, the succession commences with the Lower Menilites Formation which is represented by menilitic shales, as siliceous rocks, and bituminous calcareous shales, followed by the Lower Dysodile Formation characterized by dysodile (i.e., shale) with rare sandstone intercalations (Dumitrescu et al. 1970). The overlying Lower Kliwa Formation is dominated by thick layers of quartz-rich sandstone with rare dysodile intercalations. Locally the Lower Kliwa Formation is covered by the Upper Dysodile Formation, which is composed of dysodiles and rare sandstone intercalations (Dumitrescu et al. 1970). The overlying Podu Morii Formation is defined by calcareous sandstones intercalated with marls. The Upper Kliwa Formation is locally present and composed of friable quartz-rich sandstone. The uppermost part of the Bituminous Kliwa lithofacies is formed by the Upper Menilite Formation represented by menilitic shales and diatomites. Rarely, supra-Menilites beds are observed and contain an alternation of quartz-rich sandstone, dysodiles and occasional tuffs (Dumitrescu et al. 1970).

Sedimentation continued with deposition of a regional evaporitic level during the early Burdigalian (e.g., Ștefănescu et al. 1978; Schleder et al. 2019). The Middle Miocene (Badenian to Middle Sarmatian) succession includes different lithologies: tuffs, marls, silts, locally salt and sandstones (Ștefănescu et al. 2000). The stratigraphic succession ends with a post-tectonic cover represented by Middle Sarmatian to Recent strata (Ștefănescu et al. 2000; Schleder et al. 2019).

Study location

The diatomites of the Upper Menilite Formation are exposed in an abandoned quarry (Fig. 3). The quarry is known under several names, including Sibiciu de Sus, Pătârlagele and Burdușoaia Hill. Here, we use the name of Sibiciu de Sus when referring to the quarry. The quarry is located 2.5 km northeast from the Sibiciu de Sus city, in Buzău county (coordinates: 45°20'46.9"N, 26°22'15.3"E). Overall, the exposed
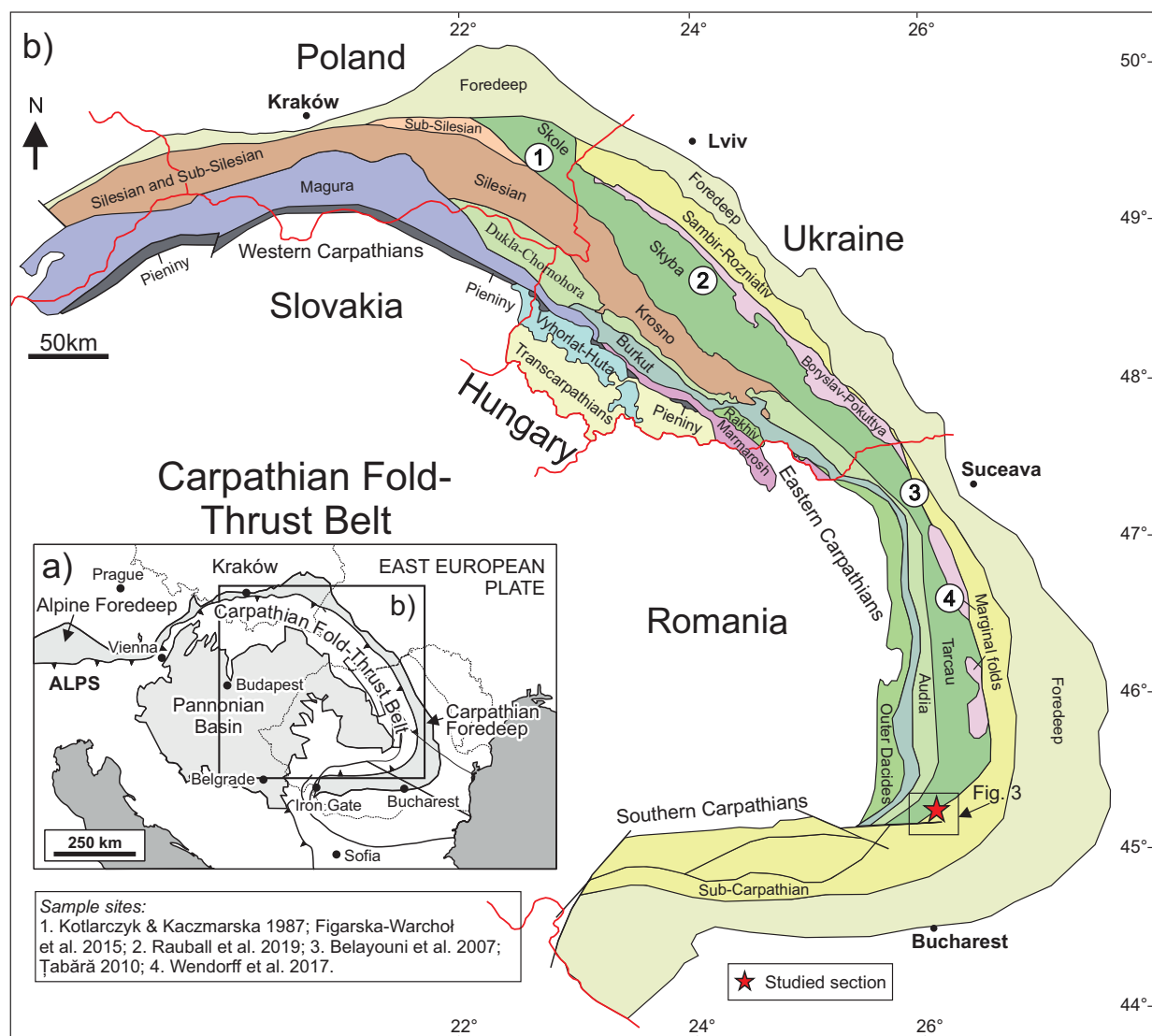
Fig. 1. a — Outline map of Central-Eastern Europe showing the location of the Carpathians. **b** — Structural map of the Carpathian fold-thrust belt with the position of the studied section and sample locations discussed in the paper. Rectangle on the main map shows the position of Fig. 3. Map redrawn after Săndulescu (1984); Glushko & Kruglov (1986); Ślączka et al. (2006).

rocks are part of a major NE–SW trending anticline, plunging to the SW. The diatomites are highly deformed both due to compressional tectonics and soft-sediment deformations. This complexity makes the lateral correlation of different layers very challenging. Vasiliu et al. (1996) and Frunzescu & Brănoiu (2004) divided the quarry into eight stratigraphic units, from bottom to top:

- **Alternation of quartz-rich sandstone and dysodile-like rocks** made up of alternations of quartz-rich sandstones, dysodiles, and locally diatomaceous shales.
- **Menilitic shales** are represented by menilitic shales (siliceous), argillaceous diatomaceous shales transitioning into diatomite. Menilitic shales have grey to black colour and are very compact with conchoidal and splintery fractures. These rocks tend to be heavier than diatomites. The two units described above are exposed in the core of the anticline and

have more than 30 m thick, are highly folded, faulted, and contain slumps and dykes.

- **Alternation of white and black diatomite** is a unit characterized by thin layers of black, organic matter-rich and whitish, organic matter-poor diatomites, heavily faulted, and it has a thickness of about 8 m and 4 m, in the SE and NW limbs, respectively.
- **Impure diatomites** are grey to blackish diatomites, with rare white laminae, with a thickness of 11 m on the SE limb and 6 m in the NW limb of the anticline.
- **Pure diatomite** is represented in the SE limb by 8 m thick pure white diatomite. The pure diatomite is changing the colour to grey at the base of the unit. The rock is fine-grained, porous and forms conchoidal fractures. The unit can reach 30 m in thickness in the NW limb of the anticline.
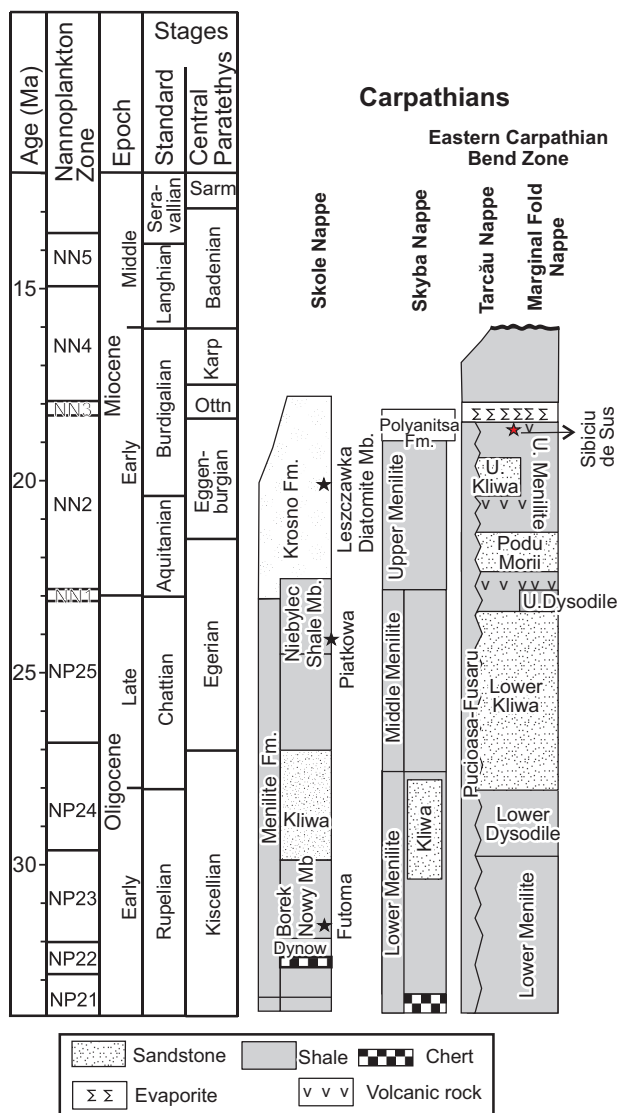
Fig. 2. Stratigraphic position of diatomite occurrences (stars) within the Carpathian realm, plotted on a simplified stratigraphy of Oligocene to Miocene (compiled from Dumitrescu et al. 1970; Kotlarczyk & Kaczmarska 1987; Ştefănescu et al. 2000; Rauball et al. 2019; Schleder et al. 2019). U. — upper.

- **Alternation of quartz-rich sandstone with diatomite** forms an approximately 20 m thick unit, and it is composed of quartz-rich sandstone beds, centimetres to metres thick and cm-thick argillaceous diatomites. Tuffaceous diatomite has been described from the NW limb. The tuffaceous diatomite has a beige-yellowish colour, is massive and has uneven fractures.

- **Breccia zone** is an approximately 12 m thick layer with mudstones, tuffs, diatomites, sandstones and micas occurring in the SE limb of the anticline. Marls with radiolaria, and marls and tuffaceous rocks with foraminifer *Globigerina* were also described.

- **Grey marls** is a unit with grey to blackish marls, about 15 m thick, and they are restricted to the SE part of the quarry.

There are layers with sandstone with some rare tuffaceous laminae.

In this study, we follow the above described nomenclature of Vasiliu et al. (1996) and Frunzescu & Brănoiu (2004), making updates only where we found it necessary.

Samples and methods

A total of 22 samples have been collected for this study from the diatomite quarry in Sibiciu de Sus. Samples S15 to S20, as well as S22, are from the upper quarry level (coordinates: 45°20'48.7"N 26°22'18.8"E), which is more than 200 m long and about 20 m high (Fig. 4). Samples S1 to S14 and sample S21 are from the lower level (coordinates: 45°20'39.2"N 26°22'13.5"E), which is about 50 m long and more than 15 m high (Fig. 5).

The mineral composition was determined with a Bruker AXS D8 Advance X-ray diffraction spectrometer (copper radiation generated at 40 kV and 40 mA). Powdered samples were carefully placed in sample holders to create a flat upper surface in order to achieve a random distribution. The different mineral phases were identified using the Diffrac.Eva software, following the method by Schultz (1964), based on peak heights. X-ray diffraction is the main technique used to determine the type of silica phase (e.g., opal-A, opal-CT). The prominent diffraction responses for opal-A are centred near ~4 Å (~22.2° 2θ) and for opal-CT at 4.09 Å (~21.75° 2θ) (Jones & Segnit 1971; Flörke et al. 1991; Smith 1998).

In order to determine organic silica content, flame atomic absorption spectroscopy was performed on all the samples using methods described by Zolitschka (1988). Approximately 100 mg sample material and 50 ml of 0.5 mol/l potassium hydroxide solution were boiled for an hour to dissolve the opaline diatom valves. Afterwards, 5 ml of the solution were diluted with distilled water (1:1). A Perkin Elmer 3030 Atom-Absorption Spectrometer was used for analysis and operated with a CH_4–N_2O flame to create free Si atoms in a gaseous state. A Si-hollow cathode lamp was used as a spectral line source. The AAS was calibrated using a Merck CertiPUR* Silicon-Standard solution (#1.1231.0500).

Total carbon (TC), total sulphur (S) and total organic carbon (TOC) contents were analysed using an ELTRA Elemental Analyser for all 22 samples. Samples for TOC measurements were decarbonized with concentrated phosphoric acid. Results are given in weight percent (wt. %). Total inorganic carbon (TIC) was determined (TIC=TC−TOC) and used to calculate calcite equivalent percentages (TIC×8.333) (e.g., Schulz et al. 2004).

Pyrolysis measurements were performed using a Rock-Eval 6 instrument. The S1 and S2 peaks (mg HC/g rock) were used to calculate the petroleum potential (S1+S2 [mg HC/g rock]), the production index (PI=S1/(S1+S2)) (Lafargue et al. 1998) and the hydrogen index (HI=S2/TOC ×100 [mg HC/g TOC]). Tmax was measured as a maturity indicator.
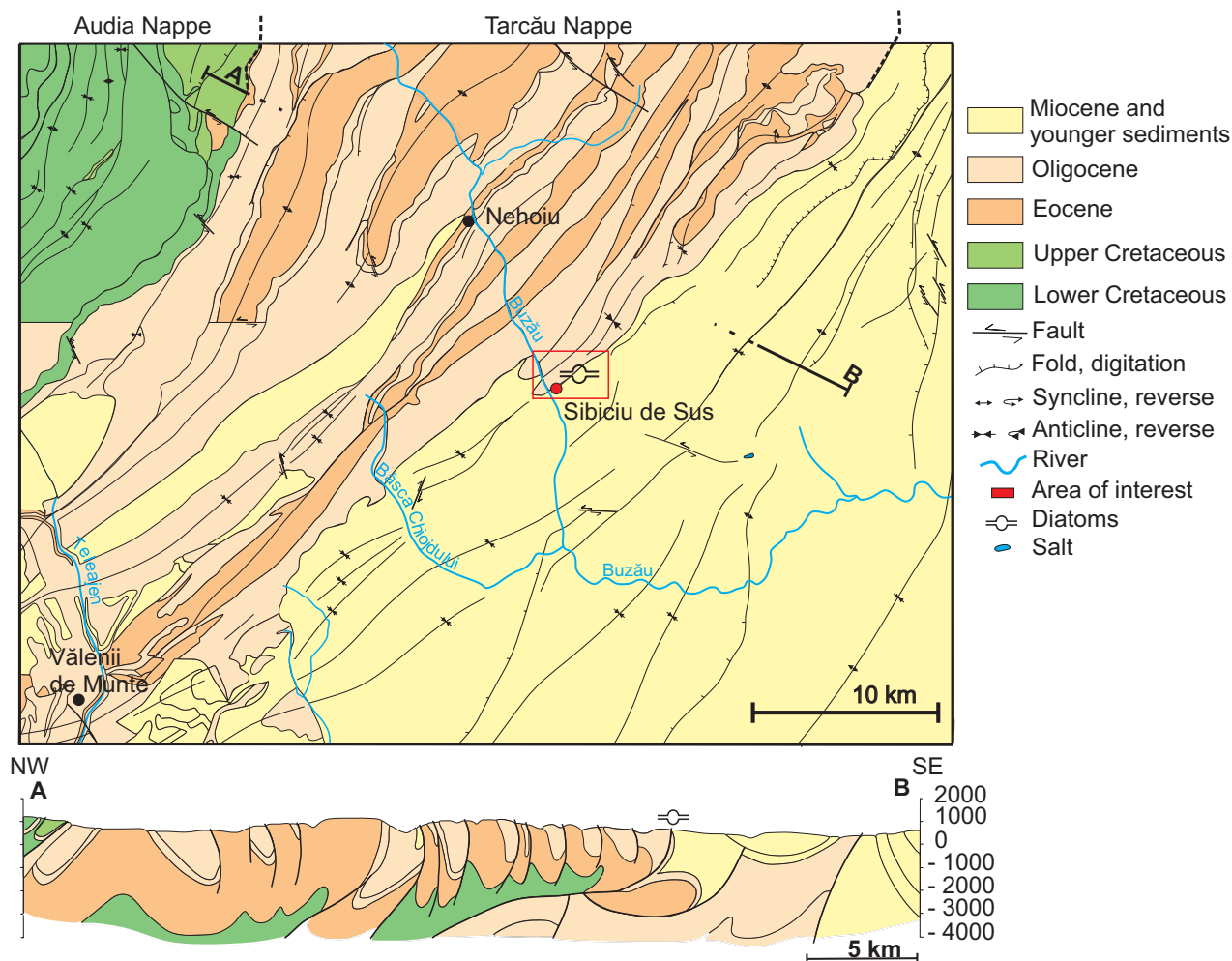
Fig. 3. Simplified geological map and cross section of the studied area (redrawn after Dumitrescu et al. 1970, sheet 29–Covasna and Moțaș et al. 1968, sheet 36–Ploiești).

Thin sections were prepared from 10 samples. They were studied using a Leica DM 2500P microscope and pictures were taken with a Leica DFC490 camera.

As the diatomite samples examined here are highly indurated, none of the commonly used methods (Dumitrică 1970; Schrader 1973) for siliceous microfossil extraction yielded positive results. The methods applied without success on 1 g of sediment in different experiments were: (1) equal amounts of hydrochloric acid (HCl) 33 % and hydrogen peroxide (H_2O_2) 33 %; (2) saturated sulphuric acid (H_2SO_4) and potassium permanganate ($KMnO_4$); (3) 1 % of hydrofluoric acid (HF) solution; (4) freezing and thawing the samples in distilled water. The duration of the treatments was varied from hours to several days, but none of the treatments yielded positive results. Therefore, no routine light microscope examination could be performed.

For micropaleontological examination, an approximately 1×1 cm piece of dry rock sample coated with gold was used. Coated rock samples were examined under the scanning electron microscope (SEM) JSM-IT100 and LEO1450P.

For the relative abundance of diatom genera, the first 300 valves were counted using the counting method described in Schrader & Gersonde (1978). The counting was done using the SEM LEO1450P at 1000× magnification.

Results

The stratigraphically lowermost rocks are exposed on the upper excavation level in the core of the anticline and include alternations of quartz-rich sandstone and menilitic shales. These rocks are overlain by cherts, alternation of white and black diatomite, and pure diatomite (Fig. 4). The lower excavation level is represented by impure diatomite (Fig. 5). Higher stratigraphic units (e.g., breccia zone, grey marls) were not accessible during the sampling campaign in 2018.

Because of strong tectonic deformation, it is impossible to determine the true thickness of the exposed units. Moreover, the relation between rocks exposed on both levels is hard to assess with confidence.

Fig. 4. Upper level of Sibiciu de Sus quarry. The white dotted lines highlight the differences in lithology and complexity of the structure. **a** — Composite picture with the position of the samples; **b** — core of the anticline represented by an alternation of quartz-rich sandstone and menilitic shales; **c** — pure diatomite (cream colour); **d** — indistinguishable layering/structure of diatomite; **e** — pure diatomite (whitish colour) and alternation of white and black diatomite.

Lithological description

The **"alternation of quartz-rich sandstone and menilitic shales"** is a heavily folded and faulted unit that comprises thin quartz-rich sandstone beds (up to 30 cm thick) and menilitic shales (5–30 cm thick) (Fig. 4). The quartz-rich sandstone is fine-grained and poorly cemented. Sulphides are abundant. Thin sections reveal the presence of angular to subangular quartz grains, minor siliceous cement and abundant glauconite grains (Fig. 6). Biotite is rare. As expected, the XRD diffractogram is dominated by quartz peaks (Fig. 7). The menilitic shales are splintery, have a dark grey to black colour when freshly broken and have a strong smell of hydrocarbons. The XRD diffractogram indicates clay minerals and quartz as the main constituents (Fig. 7). Vasiliu et al. (1996) and Frunzescu & Brănoiu (2004) described dysodile-like rocks instead of menilite. We suspect that the term dysodile was misused since our results indicate silica contents.

The unit described as **"alternation of white and black diatomite"** is composed of white and black thin layers (cm to mm thick) which are heavily faulted (Fig. 6a). The rock is compact, but relatively soft and has a very low weight. Microscopically, the rock is composed of a mass of diatom frustules embedded in the siliceous groundmass. The white layers include a lower amount of detrital grains and organic matter in comparison with the dark ones (Fig. 6b). The detrital grains are represented by angular quartz, orthoclase feldspar and glauconite.

The "**pure diatomite**" unit has a white-cream colour when freshly broken. Intercalations of white and cream diatomite laminae are visible, some of the laminae are fractured. In thin section, the pure diatomite is characterized by a mass of diatom frustules with siliceous groundmass. Some diatom frustules are intact. The detrital material is represented by angular quartz, feldspars, glauconite and volcanic glass. In thin sections, rare layers of sandy material are observed in the diatomite.
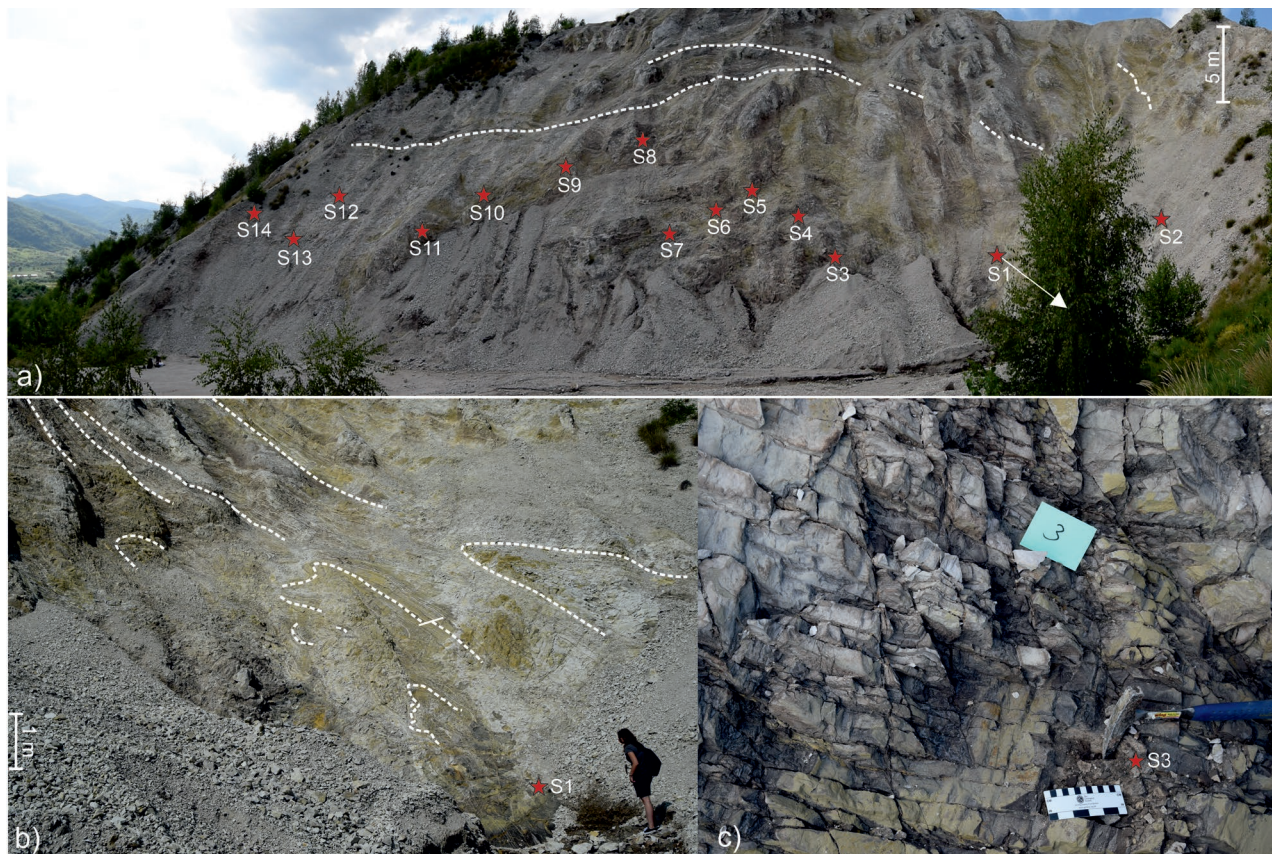
Fig. 5. The lower level of the Sibiciu de Sus quarry exposing impure diatomite. The white dotted lines highlight the complexity of the structure (**a**, **b**). The rocks are highly fractured (**c**), and note that the green-yellowish colour is caused by sulphides.

The thickness of the sandy material is variable along the observed section (Fig. 6f), indicating most probably syn-sedimentary deformation. The base of the unit is represented by strongly deformed layers represented by an alternation of white and black diatomites (>30 cm thick) (Fig. 4e).

Cherts are fine-grained, very compact without visible stratification and exhibit splintering fractures. The colour is dark grey. In thin section (Fig. 6g), the cherts show a siliceous mass with some detrital grains, including angular quartz, feldspar, sparse glauconite and rare volcanic glass.

The only lithology exposed on the lower excavation level (Fig. 5) is **impure diatomite** (fresh cut colour dark grey) which is fine-grained and compact. The rock has a very light weight and a strong hydrocarbon smell. Intercalations with white diatomite laminae are observed. Soft-sediment deformations, small fractures/faults and folds are common (Fig. 5). Sulphides are found on the surface of the samples due to weathering. In thin sections (Fig. 6d, e) abundant diatom frustules are present in a siliceous matrix. Some diatom frustules are intact and contain abundant organic matter. Detrital grains are represented by angular quartz, feldspar, glauconite and sponge spicules.

The unit designated as **"alternations of quartz-rich sandstone with diatomite"** is exposed along the southern entrance to the quarry. It is separated by vegetation from the impure

diatomites exposed at the lower level. In the field, it was hardly possible to correlate these units. The diatomaceous rock exposed here is 2 to 3 m thick and includes few sandstone layers (20 cm thick). The unit is also highly faulted, and we could not distinguish a typical depositional alternation between the sandstone and the diatomites. On a side note, Tămaș et al. (2020) demonstrated the presence of sand intrusions in a nearby outcrop of the underlying Upper Kliwa Formation. We presume that this zone might represent either a fault zone with thrusting of Upper Kliwa sandstone onto the diatomites or by sand intrusions reaching this level (or a combination of both). Unfortunately, the quality of the outcrop prevented a clear determination of the nature of the contact.

Based on XRD diffractograms, the mineral content of diatomites is rather uniform, but differences exist in opal types. Chert samples (S18, S21) contain opal-CT, whereas all other samples contain opal-A (Fig. 7). Quartz and clay minerals are also present. As expected, in the analysed menilitic shale sample (S22 in Fig. 7) opal-A was recognized, and the quartz-rich sandstone sample (S15 in Fig. 7) indicates quartz as the main mineral.

Biogenic silica (bSi) contents have been measured for all samples and are plotted in Fig. 8. Diatomites contain, on average, 51 % bSi. Lower contents are seen in the quartz-rich
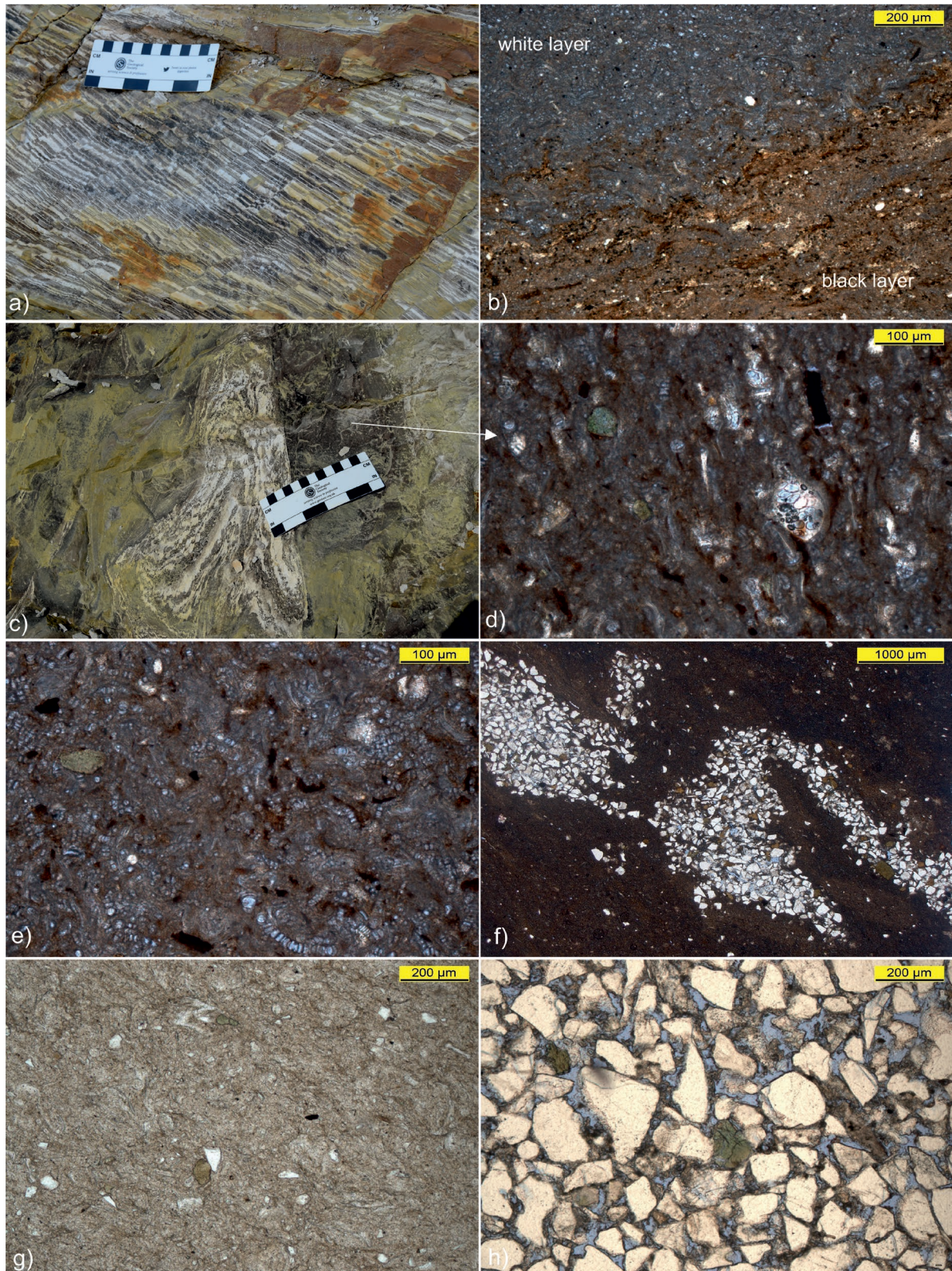
Fig. 6. Selected samples and thin-section photographs from Sibiciu de Sus quarry. **a**, **b** — Highly faulted alternation of white and black diatomite [a], the white layers contain significantly less organic matter compared with the black ones [b] (sample S17). **c**, **d**, **e** — Impure diatomite highly deformed and faulted, covered with sulphides containing abundant organic matter [c], volcanic vacuolar glass [d] (sample S1) and intact diatoms frustules [e] (sample S10). **f** — Pure diatomite with diatom mass and rare organic matter with few sandstone deformations present (sample S19). **g** — Chert with few detrital grains: angular quartz, feldspars and glauconite (sample S21). **h** — Quartz-rich sandstone containing angular quartz and glauconite with siliceous cement (sample S15).
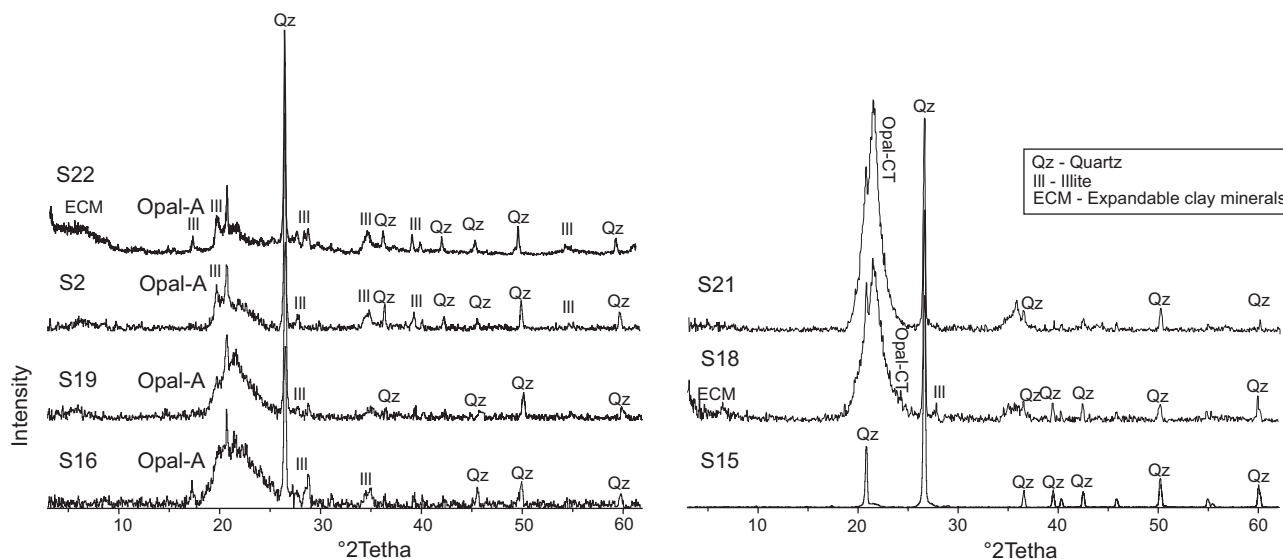
Fig. 7. Representative XRD diffractograms showing different opal types in Sibiciu de Sus samples.

sandstone (S15: 17 % bSi) and the menilitic shale (S22: 10 % bSi) samples. Carbonate contents are low in all samples, and few samples exceed 2 wt. % (Table 1, Fig. 8).

Bulk geochemical parameters

Bulk geochemical parameters measured in Sibiciu de Sus samples are listed in Table 1 and plotted in Fig. 8. The average TOC content for diatomite samples is 3.77 wt. %. Maximum TOC contents (up to 9.57 wt. %) are observed in impure diatomite samples. The menilitic shale sample also has a high TOC content (5.01 wt. %). As expected, the TOC content of the sample from quartz-rich sandstone is very low (0.36 wt. %). The sulphur (S) content follows the TOC trend but is typically much lower (average 0.42 wt. %). Therefore, TOC/S ratios are high (4–25; Fig. 8).

S2 values reach a maximum of 30.67 mg/HC g rock (Fig. 9) (avg. 14.64 mg/HC g rock), and HI values range between 206 to 515 HC/g TOC, indicating the prevalence of type II kerogen. Tmax values do not exceed 424 °C. Although Tmax values are low, the Production Index is high (0.1–0.3; Table 1; Fig. 10). This is clear evidence for the presence of migrated hydrocarbons (Fig. 10).

Diatom assemblages

Attempts to extract siliceous microfossils from diatomite samples were unsuccessful, but SEM examination enables at least a tentative insight into the taxonomic composition of the fossil diatom assemblages. The rock surfaces of eleven samples were analysed. In six samples, the diatoms were broken and/or silicified beyond recognition (Fig. 8). As light microscopic examination was impossible, most of the identifications are to the genus level. Illustrations of those diatoms for which we were able to provide a positive identification are

presented in Figs. 11–13. The average abundance of the diatom genera is plotted against the stratigraphic position of the samples examined for diatoms in Fig. 8.

Paradoxically, despite common fragmentation of diatom valves and pervasive silicification, the preservation of valve fine structure is often pristine. Diatom valves are often linked in chains, and even the most delicate areolae occlusions (i.e., vela) are preserved intact (Fig. 11b). Thus, the siliceous cement responsible for induration of the rock is unlikely to be derived from diatom dissolution.

We found two genera to be especially abundant in the Sibiciu de Sus diatom assemblages based on the average of all analysed samples: *Aulacoseira* (66 %) and *Actinocyclus* (31 %). *Ellerbeckia*, *Paralia*, *Rhaphoneis* and chrysophycean cysts have been recognized rarely, and they are represented each on average below 3 %.

A striking contrast is seen when plotting the results of the diatom genera against lithology (Fig. 8). For example, in the impure diatomite, three samples (S3, S6, S9) are heavily silicified with unidentifiable diatoms, whereas three other samples (S7, S12, S13) yield good results. Samples S7 and S13 showed similar genera abundances: *Aulacoseira* (77 % and 76 %, respectively), *Actinocyclus* (21 % and 19 %, respectively). In contrast, *Aulacoseira* (36 %) is less abundant in sample S12, which contains abundant *Actinocyclus* (61 %).

From three pure diatomite samples (S16, S19, S20), two yielded good results. Samples S16 and S19 are characterized by abundant *Aulacoseira* (56 % and 84 %, respectively) and *Actinocyclus* (39 % and 16 %, respectively).

Diatoms in sample S17, representing the black and white diatomite, are too silicified for proper identification. However, our observations show that the black layers contain significantly more diatom frustules compared to white ones. As expected, diatoms could not be detected in the sample from the quartz-rich sandstone.
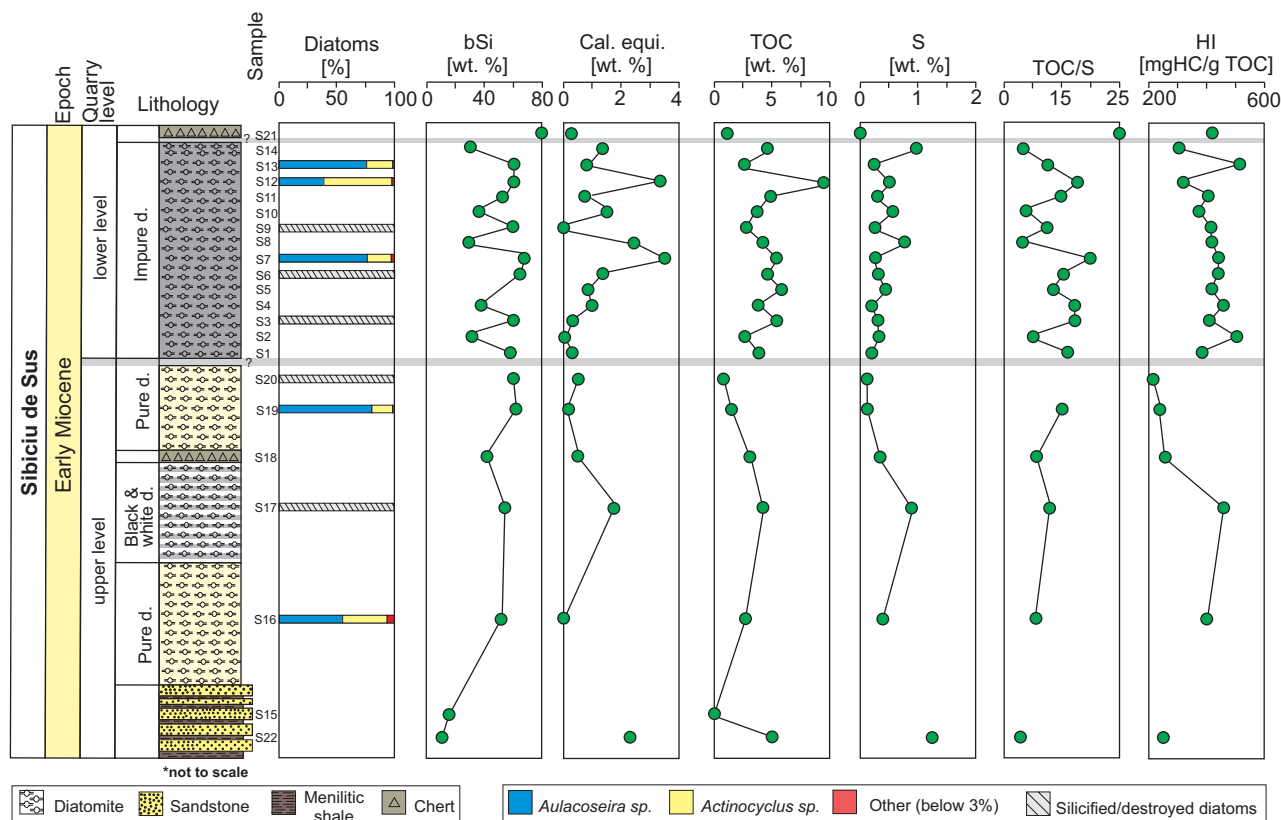
Fig. 8. Bulk geochemical parameters and the relative abundance of the prevalent diatom genera of the diatomites exposed at Sibiciu de Sus. bSi — biogenic silica; Cal. equi. — calcite equivalent; TOC — total organic carbon; S — total sulfur; HI — hydrogen index.

Discussion

Maturity, migrated bitumen and hydrocarbon source rock potential

Tmax values of the diatomites from Sibiciu de Sus (max. 424 °C) indicate that the studied section is immature. Nevertheless, S1 and PI values are high. This shows the presence of migrated bitumen (Fig. 10), which is also responsible for the strong hydrocarbon smell of many diatomite samples.

In order to test the influence of the migrated bitumen on the Rock-Eval results, a cm-size piece and several mm-size fragments from sample S12 were washed with hexane. The obtained S1 values were reduced by 50 % (cm-size sample; PI: 0.09) and 75 % (mm-fragments; PI: 0.05), respectively. The S2 values decreased by a maximum of 5 %, implying that the influence on S2 and HI is minor. Hence, the organic matter of most diatomite samples is classified as oil-prone type II kerogen (Fig. 9). Only pure diatomite, chert and menilitic shales contain a type III–II kerogen.

The generative potential is determined based on TOC and the petroleum potential (S1+S2). Based on the TOC contents, all fine-grained Sibiciu de Sus samples, except for pure diatomite samples (S19, S20), may be classified as a very good source rock (Fig. 14). Based on the petroleum potential,

most samples are classified as good to very good source rocks (irrespective if original or corrected S1 values are taken into consideration).

In order to approximate the amount of hydrocarbons (in tons HC) that can be generated beneath 1 m² of surface area, the source potential index is determined (SPI=thickness× (S1+S2)×bulk density/1000; Demaison & Huizinga 1994). Due to the highly deformed structure of the rock unit exposed at Sibiciu de Sus, we use a net thickness of the diatomite to 40 m, based on the measurements by Frunzescu & Branoiu (2004), for the calculation of the SPI. Considering the shallow burial depth, and the high amount of diatoms, a density of only 1.95 g/cm³ has been applied. The average S1 values (of 3.83 mg HC/g rock) is clearly influenced by migrated bitumen. For our calculation, we consider only 25 % of it (0.96 mg HC/g rock) and the average S2 of 15.54 mg HC/g rock. Using these data, the SPI is calculated as 1.3 t HC/m².

Depositional environment

Diatoms can be excellent environmental indicators. A reliable assessment of the depositional environment, however, relies on the proper taxonomic identification, which has been considerably hindered by the pervasive silicification encountered in this study. In Sibiciu de Sus, previous work on diatoms by Frunzescu & Brănoiu (2004) identified *Actinocyclus*,

Table 1: Bulk parameters for analysed samples from Sibiciu de Sus quarry.

Sample	S1 [mg HC/g]	S2 [mg HC/g]	Tmax [°C]	TOC [%]	S [%]	PI	HI [mg HC/g TOC]	TOC/S	Calc. Equiv. [%]
Impure diatomite									
S21	0.30	4.35	422	1.04	0.04	0.06	419	24.8	0.39
S14	4.57	14.07	417	4.59	0.92	0.25	307	5.0	1.33
S13	3.29	13.69	423	2.66	0.24	0.19	515	11.0	0.78
S12	5.56	30.67	419	9.57	0.52	0.15	320	18.5	3.36
S11	2.61	19.95	423	4.88	0.33	0.12	409	14.8	0.72
S10	6.59	13.71	414	3.70	0.59	0.32	370	6.3	1.69
S9	1.39	11.67	422	2.81	0.25	0.11	415	11.1	0.03
S8	8.29	16.69	413	4.01	0.72	0.33	417	5.6	2.33
S7	8.84	23.64	418	5.30	0.26	0.27	446	20.1	3.41
S6	4.46	20.75	421	4.69	0.30	0.18	443	15.5	1.35
S5	3.28	24.03	422	5.78	0.42	0.12	416	13.7	0.97
S4	4.02	17.65	420	3.85	0.22	0.19	458	17.2	1.00
S3	5.33	21.80	420	5.33	0.31	0.20	409	17.2	0.31
S2	2.02	13.19	420	2.61	0.34	0.13	505	7.7	0.05
S1	2.45	13.96	421	3.61	0.23	0.15	387	15.6	0.35
Pure diatomite and chert									
S20	0.20	1.77	415	0.86	0.10	0.10	206	8.4	0.52
S19	0.28	2.73	417	1.22	0.10	0.09	224	12.6	0.11
S18	0.58	7.68	414	2.90	0.34	0.07	265	8.5	0.50
Black and white diatomite									
S17	6.50	12.27	416	3.43	0.85	0.35	358	4,1	1.80
Pure Diatomite									
S16	0.72	10.55	424	2.64	0.38	0.06	400	7.0	0.00
Quartz-rich sandstone and menilitic shale									
S15				0.36	0.22				
S22	2.44	12.58	419	5.01	1.42	0.16	251	3.5	2.18

TOC — total organic carbon, S — Sulphur, HI — hydrogen index, PI — production index, calc. equi. — calcite equivalent.

Coscinodiscus, *Melosira* and *Stephanodiscus*, and Sebe-Rădoi et al. (2017) reported *Actinocyclus, Coscinodiscus* and *Actinoptychus* as the dominant genera. Presently, some of these diatom genera are undergoing taxonomic revision. For example, numerous taxa originally described as *Melosira* spp. have been transferred elsewhere, including *Aulacoseira*, *Paralia*, *Orthoseira* and *Ellerbeckia* (Round et al. 1990). The taxa reported as *Melosira clavigera* and *M. granulata* tentatively identified by Frunzescu & Brănoiu (2004) from Sibiciu de Sus have been transferred to *Ellerbeckia* and *Aulacoseira*, respectively (Simonsen 1979; Crawford & Sims 2006). Also, the taxonomy of the fossil species of *Coscinodiscus* is poorly resolved, with some taxa transferred to other genera, especially *Actinocyclus* (e.g., Bradbury & Krebs 1995).

In the present study, the most abundant genus is the freshwater diatom *Aulacoseira*. In the Western Carpathians (Slovakia), specifically in the lacustrine Turiec Basin, *Aulacoseira turiecensis* was described by Ognjanova-Rumenova & Pipík (2018) in a shallow littoral zone with a salinity range of 0.2–0.3 ‰ (Ognjanova-Rumenova & Pipík 2015, 2018). In the Transylvanian Basin *Aulacoseira temperei* was described in Neogene lacustrine sediments (e.g., Ognjanova-Rumenova & Crawford 2012). Further, the Holocene *Aulacoseira* can indicate shallow-water conditions with

high wind exposure, which provides the turbulent, high-nutrient regime favourable for this taxon to flourish (Kociolek et al. 2015).

Actinocyclus is a genus of both marine and non-marine diatoms (Round et al. 1990). It is a common component of the phytoplankton found in Neogene lacustrine diatomaceous sediments in the Western United States (Bradbury & Krebs 1995). In Europe, *Actinocyclus* is documented in Neogene sediments as a freshwater species and it was described in the Ukrainian part of the Eastern Paratethys (Olshtynska 2001), in the Taman Peninsula (Radionova & Golovina 2011) and further east in the Vitim Plateau, Russia (Usoltseva et al. 2010). Strictly marine diatoms are less abundant in Sibiciu de Sus, and are mostly represented by *Paralia* and *Rhaphoneis*.

Sebe-Rădoi et al. (2017) interpreted a shallow marine depositional environment with freshwater contribution for Sibiciu de Sus. In the present study, however, the high percentages of predominantly freshwater genera such as *Aulacoseira* and *Ellerbeckia*, and taxa characteristic of both marine and non-marine settings such as *Actinocyclus*, point to a brackish-water environment. At the time of deposition, the conditions were probably highly eutrophic for the diatoms to thrive. The high diatom production in Sibiciu de Sus may have been sustained by river plumes, which are usually strongly
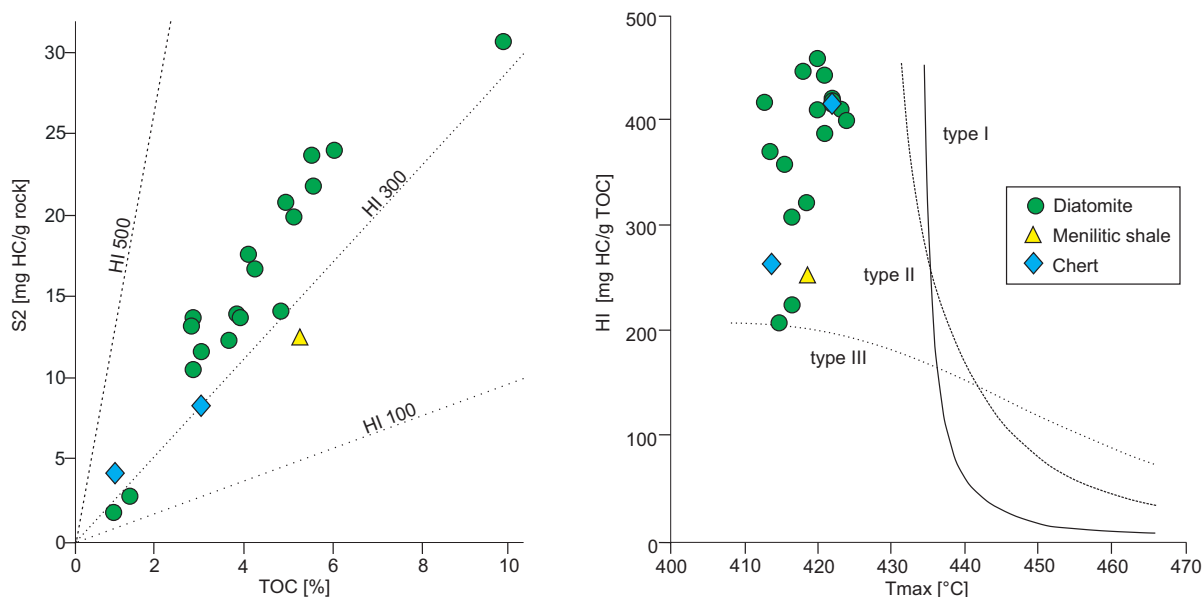
Fig. 9. Plots of S2 vs TOC and Hydrogen Index (HI) vs. Tmax for Sibiciu de Sus quarry samples.

eutrophicated (e.g., Lohrenz et al. 1990; Smith & Demaster 1996). It should be noted, however, that these observations are based on SEM examination of fresh rock surfaces, and that the diatom assemblage composition could differ when examined in LM following chemical extraction of siliceous microfossils.

The above interpretation is supported by the high TOC/S ratio which points toward a nonmarine depositional environment. Additionally, the presence of glauconite is usually an indication for shallow marine environment (Smith & Hiscott 1987) and a slow rate of deposition (Triplehorn 1965).

Additionally, the glauconite from the Sibiciu de Sus is most probably detrital since it is considered unlikely for the glauconite to form in estuaries or at water depths shallower than 15 m due to wave-induced turbulence (e.g., Cloud 1955; Rothwell 1989).

Fig. 10. Plot of Tmax vs. Production Index which indicate that the samples from Sibiciu de Sus quarry are contaminated with migrated hydrocarbons.

Regional significance

Diatom preservation

The diatomites at Sibiciu de Sus likely represent a shallow brackish nearshore depositional setting. The section contains abundant well-preserved diatoms, represented by several genera. The excellent preservation of the valve fine structure in the diatoms suggest that silica content was high, preventing the diatom frustules from getting dissolved. Hence, volcanic activity in the area should not be excluded considering that tuffs have been previously described in the quarry (Vasiliu et
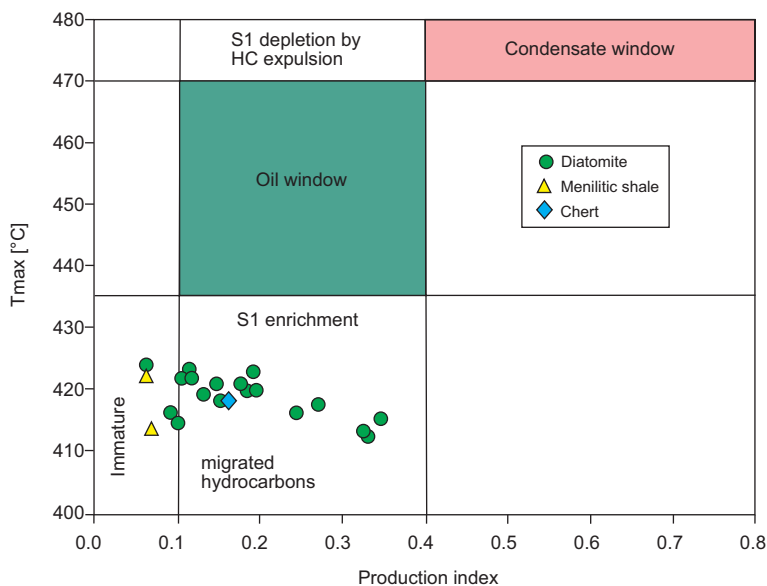
al. 1996; Frunzescu & Brănoiu 2004). Volcanic tephra significantly buffers diatom preservation (Harper et al. 2015), which might be the case in Sibiciu de Sus diatom preservation.

The remarkably good preservation of the diatoms and the considerable thickness of the diatomite deposits make Sibiciu de Sus unique compared with other Oligo–Miocene diatomaceous successions in the Carpathian realm. For example, within the Skole Nappe in Poland diatomites are present in three horizons (e.g., Kotlarczyk & Kaczmarska 1987): Futoma Member (Lower Oligocene; Menilite Formation), Piątkowa horizon (Upper Oligocene, Lower Miocene, at the transition between Menilite and Krosno Formations) and Leszczawka
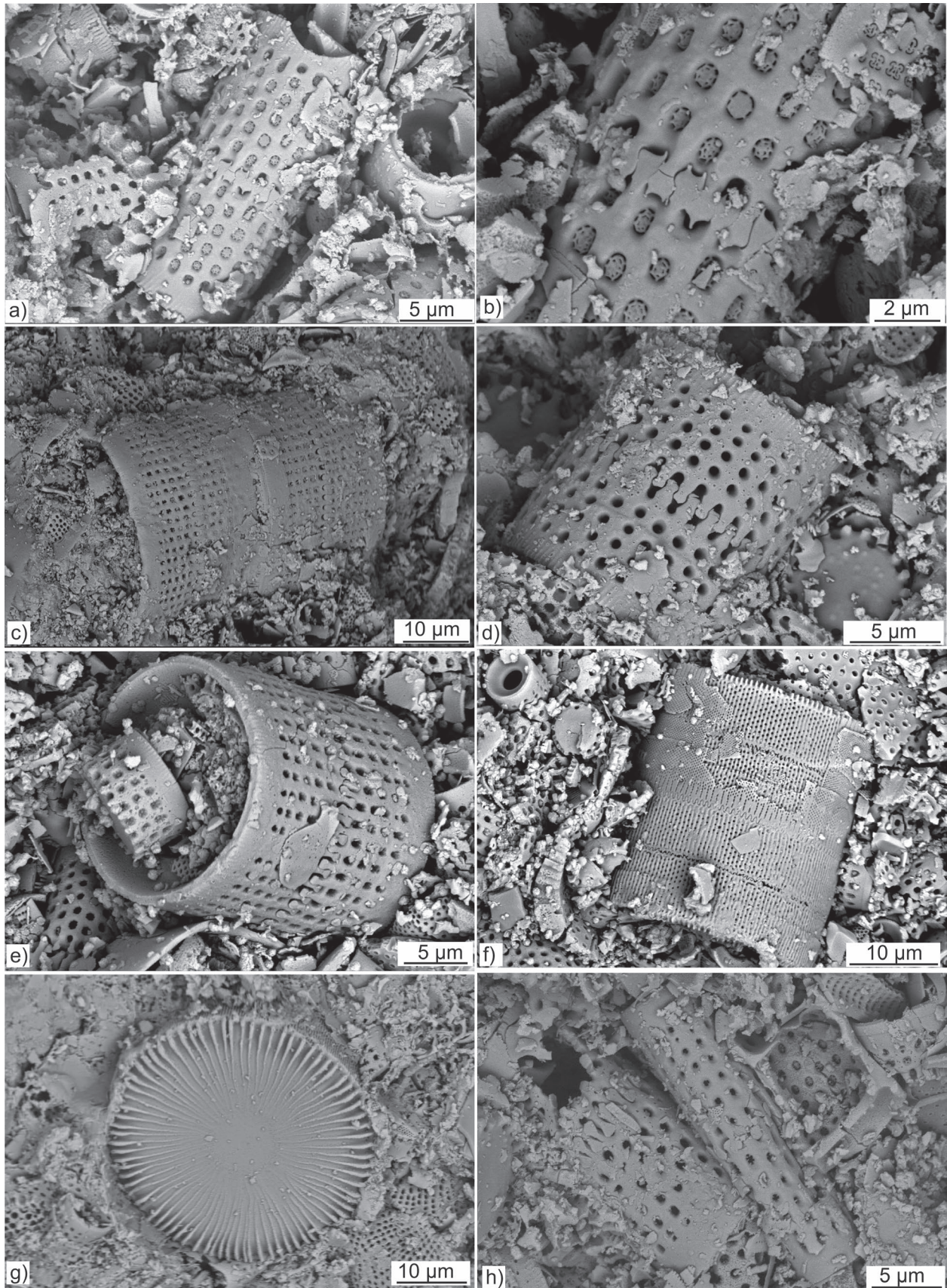
Fig. 11. SEM photographs of diatoms from Sibiciu de Sus quarry: **a**, **b** — *Aulacoseira aff. temperei* Ognjanova-Rumenova & Crawford (2012); **c**, **d**, **e** — *Aulacoseira* sp.; **f**, **g** — *Ellerbeckia*; **h** — *Aulacoseira* sp..
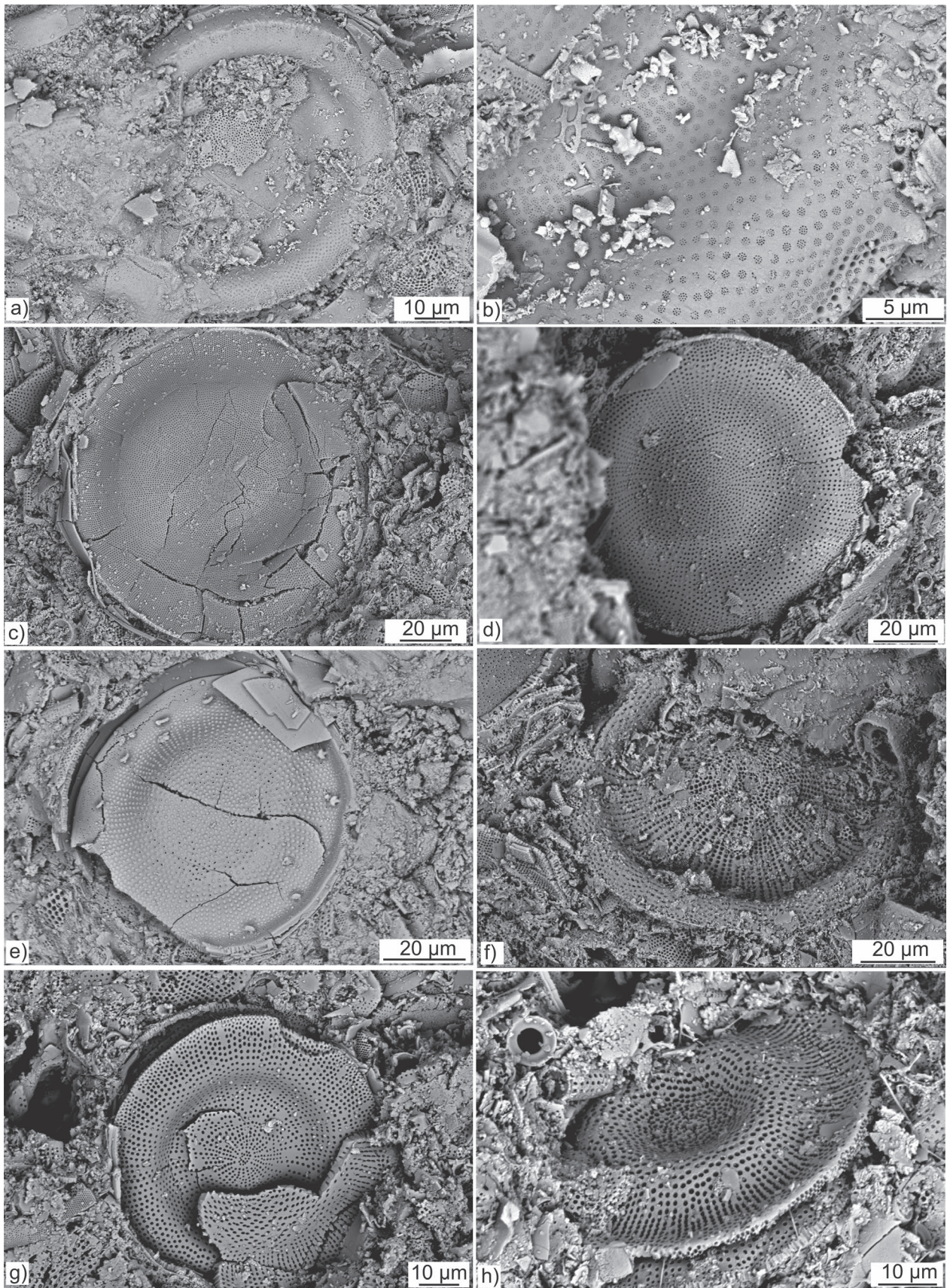
Fig. 12. SEM photographs of a variety of *Actinocyclus* spp. (**a–h**) observed in Sibiciu de Sus diatomites.
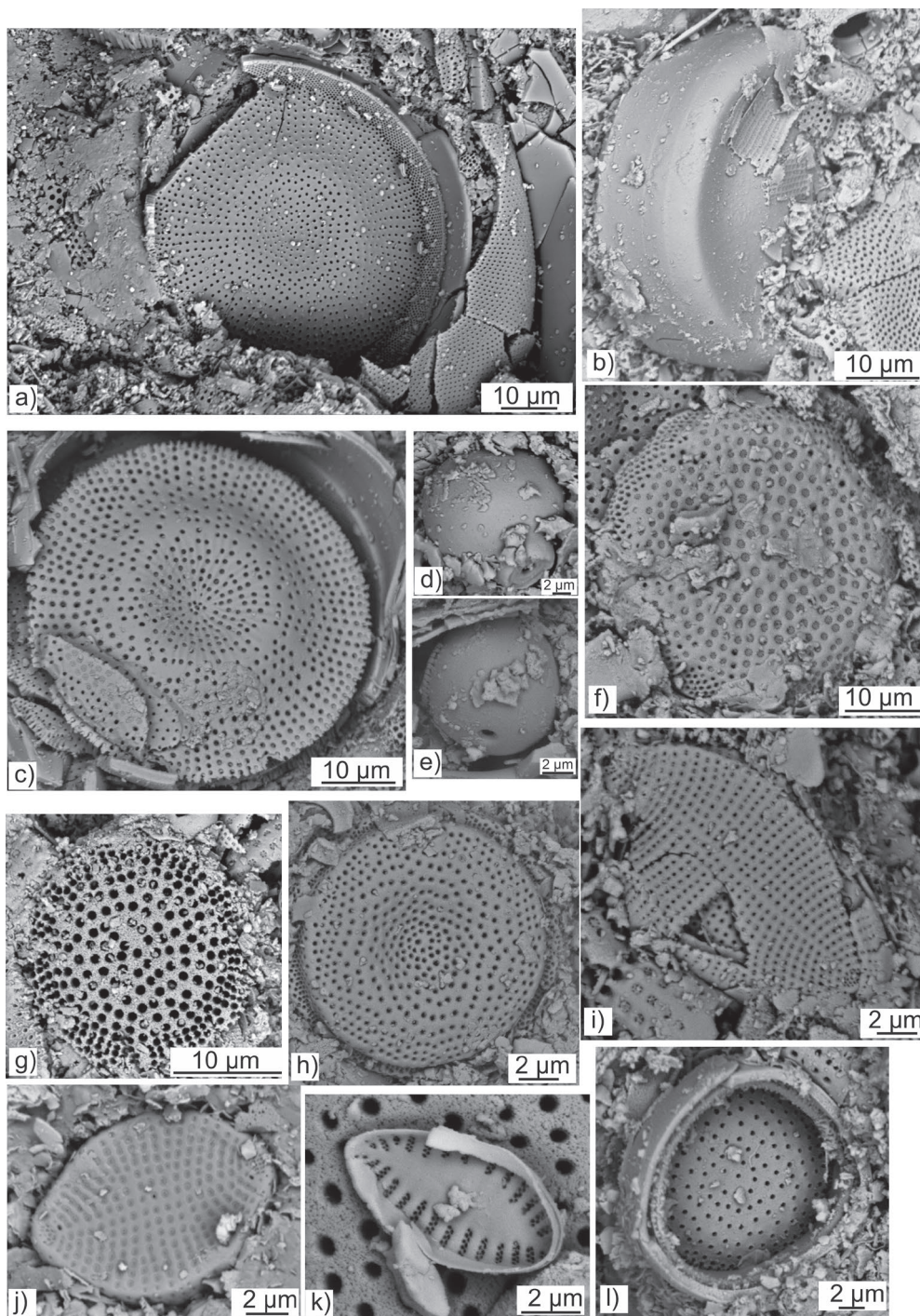
Fig. 13. SEM photographs of diatoms from Sibiciu de Sus quarry: **a**, **b** — *Actinocyclus* sp.; **c** — unidentified diatom; **d**, **e** — chrysophyte cysts; **f**, **g**, **h** — unidentified diatom; i, j — *Rhaphoneis* cf. *Rh. amphiceros*; k, l — unidentified diatom.

Diatomite Member (Lower Miocene; Strzyżów Formation; formerly Upper Krosno Formation) (Fig. 2). The sedimentary beds are largely represented by diatomites, diatomaceous shales, shales, sandstones, cherts and tuffite deposited in a shallow marine, neritic environment. The diatomite thickness varies significantly, from approximately 10 m in the Futoma Member, 3 to 25 cm intercalations in Piątkowa and a complex of up to 140 m in Leszczawka Diatomite Member (Kotlarczyk

& Kaczmarska 1987; Figarska-Warchoł et al. 2015 and references therein).

Although the diatomites from the Menilite and Krosno formations contain more shale compared with Sibiciu de Sus, the diatoms are as strongly indurated as at Sibiciu de Sus. Kotlarczyk & Kaczmarska (1987) spent months on the preparation of the samples in order to achieve a positive identification of the diatoms. Later, Figarska-Warchoł et al. (2015)

observed the rock samples using SEM, but the diatoms have mostly broken frustules.

Petroleum potential comparison

In general, the Oligocene to Lower Miocene Menilite Formation comprises menilitic shales, bituminous marls and black shales. It is widespread in the Carpathians, and it forms the most important hydrocarbon source rock (e.g., Kotarba & Koltun 2006; Boote et al. 2018). Sachsenhofer et al. (2015) and Rauball et al. (2019) studied the vertical variation of the source potential of the Lower Menilites and the Upper Menilites in the Eastern Carpathians (Fig. 2). An overview of the Menilite Formation is given by Sachsenhofer et al. (2018a,b).

In the ECBZ, the extent of Upper Menilites is limited, and they have been described mostly in the southern part (Slănicul de Buzău river valley; Mutihac & Ionesi 1974). Overall, geochemical data from the Tarcău Nappe are insufficient for estimating the hydrocarbon potential of the Upper Menilites. For example, Grasu et al. (1988) provided a percentage ranging from 0 to more than 20 % TOC, although no location for the analysed samples is provided. Țabără (2010) postulated only the TOC ranges (2.25–11.85 % TOC) for the samples analysed in the north side of the Tarcău Nappe (near Gura Humorului, see Fig. 1 for location). However, the data provided is still insufficient for a proper assessment of the Upper Menilites hydrocarbon potential within the Tarcău Nappe and additional studies are necessary.

It is worth mentioning that the Upper Menilites have been described in the northern part of the Carpathians, specifically in the Skyba Nappe in Ukraine (corresponding to Tarcău Nappe in Romania). Here, the TOC content of the Upper Menilites is moderately high (2–7 wt. %; max. 15 %) and the HI values are on average 440 mg HC/g TOC. On average, the values for S1 is 0.45 mg HC/g rock, S2 is 32.30 mg HC/g rock and Tmax is 425 °C (Rauball et al. 2019). Overall, the petroleum potential of the Upper Menilites is good to very good (Fig. 14). The organic matter is immature (Rauball et al. 2019). Sachsenhofer et al. (2015) studied the "Upper Dysodilic Shale Member", representing the Upper Menilites in the Marginal Folds Nappe, and estimated the SPI as 1.82 t HC/m².

In comparison, the Lower Menilites represented in the Tarcău Nappe have a very good hydrocarbon potential (Fig. 14), and only few samples display poor hydrocarbon potential. The samples from the Kliwa lithofacies presented by Belayouni et al. (2007) have a fair to good hydrocarbon potential, and the samples from Tărcuța Creek (Wendorff et al. 2017) have poor to good potential (Fig. 14). The TOC maximum reached 10.99 wt. % in the Kliwa lithofacies (avg. 2.87 wt. %), and in Tărcuța Creek it is 2.58 wt. % (avg. 1.74 wt. %). The HI is on average 285 mg HC/g TOC for the Kliwa lithofacies (Belayouni et al. 2007) and 384 mg HC/g TOC for Tărcuța Creek (Wendorff et al. 2017). From the two sections, only the last one is thermally mature.

Moreover, Lower Menilites from the Skyba Nappe contain TOC in excess of 20 wt. % and the HI values are very high (up to 800 mg HC/g TOC). This highlights the excellent hydrocarbon potential of the thermally immature succession (Rauball et al. 2019).

Regional understanding

During Early Miocene, the connection between the Central and Eastern Paratethys was closing (e.g., Rögl 1999; Kováč et al. 2018). The tectonic movements and the uplift of
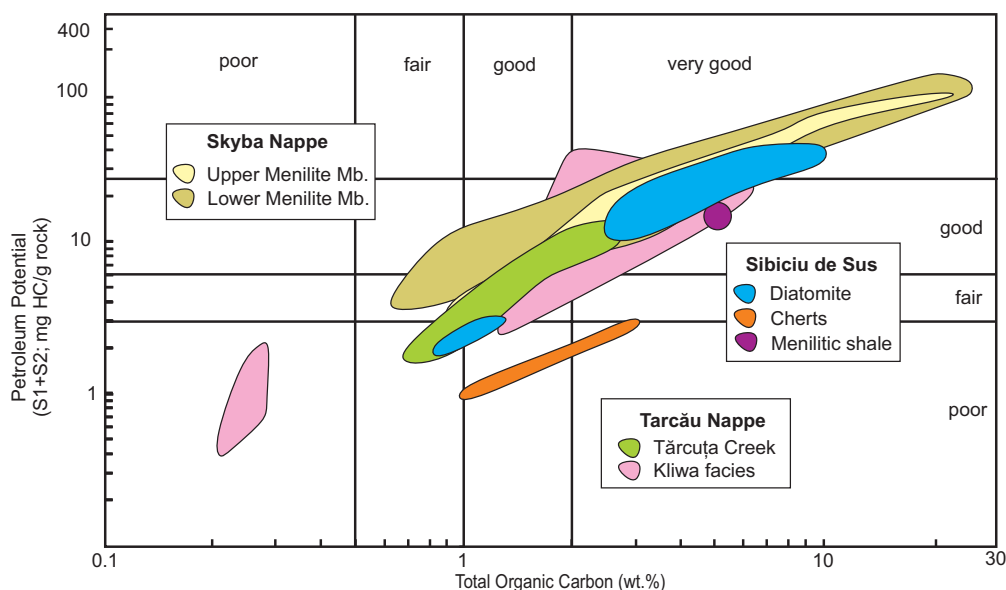

Fig. 14. Petroleum potential of the diatomites from Sibiciu de Sus. Values of the petroleum potential of equivalent sediments in the Tarcău Nappe and Skyba Nappe (Ukraine) are shown for comparison (data compiled from Belayouni et al. 2007; Wendorff et al. 2017; Rauball et al. 2019).

the Carpathians caused changes in the sedimentary regimes. In the Carpathian Basin, the marine connection was obstructed and evaporites were deposited in the Romanian and Ukrainian sectors across the NN3/NN4 nannofossil zone boundary (Rögl 1999; Popov et al. 2004; Gozhyk et al. 2015). The last anoxic event within the basin is represented by the Upper Kliwa sandstone and Upper Menilites, which indicates rapid changes between open marine and restricted marine anoxic conditions (Amadori et al. 2012). The rapid changes can be observed from the marine Upper Kliwa sandstone to the brackish Upper Menilites (i.e., Sibiciu de Sus diatomites). For example, 50 km east from Sibiciu de Sus, in Telega Valley and Vălenii de Munte (Prahova County), siliceous microfossils were documented in the Upper Kliwa sandstone by Dumitrică (1989, 1995). The diatoms are represented in the lower part by *Actinoptychus thumii* (Schmidt) Hanna, *Coscinodiscus oculus irodis* Ehr., *Melosira clavigera* Gron, *Rhaphoneis gemmifera* Ehr., *R. paralis* Hanna, *R. rhombica* Ehr. and *Triceratium condeconum* Bail and in the upper part by *Coscinodiscus grunowii* Part., *Stephanodiscus hanitai* Grunn and *Aulacoseira praegranulata* Jousé. Silicoflagelate taxa reported by Dumitrică (1989; 1995) include *Corbisena flexuosa*, *C. bimucronata* s.l., *Naviculopsis navicula* and *N. quadrata*.

Moreover, the Sibiciu de Sus diatomites display the depositional sequence during the closure or after the marine connection was closed between the Eastern and Central Paratethys, and before deposition of the Ottnangian evaporitic sequence. Besides, the sediments are strongly deformed due to compressional tectonics and soft-sediment deformation.

The Oligocene and Lower Miocene in the Romanian Carpathians contain endemic fossil assemblages which makes the age determination constrained and uncertain (e.g., Melinte-Dobrinescu & Brustur 2008; Munteanu et al. 2014; Bercea et al. 2016; Tămaş 2018).

For example, the Lower Kliwa sandstone is presumed to be Chattian (Oligocene) in age within the ECBZ (e.g., Dumitrescu et al. 1970; Săndulescu 1984; Schleder et al. 2019) and in the northern part of the Tarcău Nappe, the formation age is proposed to be Aquitanian (Miocene) (Belayouni et al. 2007). Moreover, age estimations have been made on the Upper Kliwa sandstone from the Buzău Valley based on the silicoflagellates and the diatom assemblages to Aquitanian–Burdigalian (Dumitrică 1989; 1995). Sibiciu de Sus outcrop represents another location within the ECBZ where a certain age cannot be provided. However, given the regional context and the previous studies, the Upper Menilites studied here are most probably Lower Burdigalian in age and cannot be younger than the evaporitic sequence above (i.e. intra-Burdigalian salt; Schleder et al. 2019).

Conclusions

The abandoned Sibiciu de Sus quarry provides one of the largest exposures of diatomites in the Eastern Carpathians. The exposed diatomites represent the upper part of the Upper

Menilites in the ECBZ. The diatomites, represented here by several lithologies, are highly deformed due to soft-sediment deformation and subsequent compressional tectonics.

The Sibiciu de Sus diatomites are characterized by well-preserved diatom assemblages, where even the most delicate areolae occlusions are preserved intact. However, the samples are highly indurated and common diatom extraction methods yielded no positive results. Therefore, diatom assemblages were examined using SEM techniques. Diatom assemblages are represented by two dominant genera (*Aulacoseira, Actinocyclus*) and three subordinate genera (*Ellerbeckia*, *Paralia*, *Rhaphoneis*) and suggest deposition in a nearshore brackish environment.

The hydrocarbon potential of the Lower Miocene rocks is good to very good, with an average TOC of 3.77 wt. % and type II–III kerogen (avg. HI: 384 mg HC/g TOC). The organic matter is thermally immature. However, high amounts of S1 hydrocarbons provide proof of the presence of migrated hydrocarbons. The SPI calculations indicate that the exposed section could generate about 1.3 t HC/m² if mature.

References

Amadori M.L., Belayouni H., Guerrera F., Martín-Martín M., Martin-Rojas I., Miclăuş C. & Raffaelli G. 2012: New data on the Vrancea Nappe Moldavidian Basin, Outer Carpathian Domain, Romania: paleogeographic and geodynamic reconstructions. *International Journal of Earth Sciences* 101, 1599–1623. https://doi.org/10.1007/s00531-011-0744-1

Bazhenova O.K. 2002: Oil and gas source rock potential and the presence of oil and gas in Sakhalin. In: Gladenkov Y.B., Bazhenova O.K., Grechin V.I., Margulis L.S. & Salnikov B.A. (Eds.): The Cenozoic geology and the oil and gas presence in Sakhalin. *GEOS,* Moscow, 137–194 (in Russian).

Belayouni H., Di Staso A., Guerrera F., Martín Martín M., Miclăuş C., Serrano F. & Tramontana M. 2007: Stratigraphic and geochemical study of the organic-rich black shales in the Tarcău Nappe of the Moldavidian Domain Carpathian Chain, Romania. *International Journal of Earth Sciences* 98, 157–176. https://doi.org/10.1007/s00531-007-0226-7

Bercea R., Balc R., Filipescu S., Zaharia L. & Pop S. 2016: Middle Miocene micropaleontological and sedimentary aspects within a piggy-back basin, Pucioasa section, Carpathian Bend Zone, Romania. *AAPG European regional conference and exhibition*, Bucharest, Abstract Book, 50.

Boote D.R.D., Sachsenhofer R.F., Tari G. & Arbouille D. 2018: Petroleum provinces of the Paratethyan region. *Journal of Petroleum Geology* 41, 247–298. https://doi.org/10.1111/jpg.12703

Bradbury J.P. & Krebs W.N. 1995: The diatom genus *Actinocyclus* in the Western United States. U.S. *Geological Survey Professional Paper* 1543-AB, 1–68. https://doi.org/10.3133/pp1543AB

Cloud P.E. 1955: Physical limits of glauconite formation. *AAPG Bulletin* 39, 484–492.

Crawford R. & Sims P.A. 2006: The diatoms *Radialiplicata sol* (Ehrenberg) Glezer and *R. clavigera* (Grunow) Glezer and their transfer to *Ellerbeckia* Crawford, thus a genus with freshwater and marine representatives. *Nova Hedwigia* Beiheft 130, 137–162.

Demaison G. & Huizinga B.J. 1994: Genetic classification of petroleum systems using three factors: charge, migration and entrapment. *AAPG Memoir* 60, 73–92.

Dicea O. 1996: Tectonic setting and hydrocarbon habitat of the Romanian external Carpathians. In Ziegler P.A. & Horvath F. (Eds.): Peri-Tethys Memoir 2. Structure and prospects of Alpine basins and forelands. *Memoires du Museum National d'Histoire Naturelle* Paris 170, 403–425.

Dumitrescu I., Săndulescu M., Bandrabur T. & Săndulescu J. 1970: Geological map L-35-XV, sheet 29 Covasna 1:200,000 [Harta geologică L-35-XV, foaia 29 Covasna 1:200,000]. *Institutul Geologic al României*, Bucureşti.

Dumitrică P. 1970: Cryptocephalic and cryptothoracic *Nassellaria* in some Mesozoic deposits of Romania. *Cercetari de Geologie, Geofizica, Geografie, Seria Geologie* 14, 45–124.

Dumitrică P. 1989: Siliceous microfossils from the Upper Kliwa Sandstone (Preliminary results). In: The Oligocene from the Transylvanian Basin. Romania volume, *Editura Suraru*, Cluj-Napoca, 249–254.

Dumitrică P. 1995: Lower Miocene siliceous microfossils from the Bending Zone of the Eastern Carpathians. *Romanian Journal of Stratigraphy* 76, 27–29.

Figarska-Warchoł B., Stańczak G., Rembiś M. & Toboła T. 2015: Diatomaceous rocks of the Jawornik deposit the Polish Outer Carpathians – petrophysical and petrographical evaluation. *Geology, Geophysics & Environment* 41, 311. https://doi.org/10.7494/geol.2015.41.4.311

Flörke O.W., Graetsch H., Röller K., Martin B. & Wirth R. 1991: Nomenclature of micro-and non-crystalline silica minerals. *Neues Jahrbuch für Mineralogie*, *Abhandlungen* 163, 19–42.

Frunzescu D. & Brănoiu G. 2004: Geological monograph of the Buzău River Basin [Monografia geologică a Bazinului râului Buzău]. *Editura Universităţii din Ploieşti*, 1–458 (in Romanian).

Glushko W.W. & Kruglov S.S. 1986: Tectonic map of the Ukrainian Carpathians, scale 1:200,000, 6 sheets. *Ministerstvo Geologii*, Kiev.

Gozhyk P., Semenenko V., Andreeva-Grigorovich A. & Maslun N. 2015: The correlation of the Neogene of Central and Eastern Paratethys segments of Ukraine with the International Stratigraphic Chart based on planktonic microfossils. *Geologica Carpathica* 66, 235–244. https://doi.org/10.1515/geoca-2015-0022

Grasu C., Catană C. & Grinea D. 1988: Carpathian flysch – Petrography and economic considerations [Flişul Carpatic – Petrografie şi consideraţii economice]. *Editura Tehnică*. Bucureşti, 1–208 (in Romanian).

Grasu C., Miclăuş C., Florea F. & Şaramet M. 2007: Geology and economic use of bituminous rocks of Romania. *Univ.Al. I. Cuza*, Iaşi, 1–253.

Grigoraş N. 1955: Comparative study of Paleogene facies between Putna and Buzău [Studiul comparativ al faciesurilor Paleogenului dintre Putna şi Buzău]. *Anuarul Comitetului Geologic* 28, 99–220 (in Romanian).

Hajós M.A. 1968: Die Diatomeen der Miozanen Ablagerungen des Matravorlandes. *Geologica Hungarica* 37, 1–401.

Hajós M.A. 1986: Stratigraphy of Hungary's Miocene diatomite deposits [Magyarországi miocén diatomás képzödmények rétegtana]. *Institutum Geologicum Hungaricum Series Paleontologica* 49, 1–339 (in Hungarian).

Harper M.A., Pledger S.A., Smith E.G.C., Van Eaton A.R. & Wilson C.J.N. 2015: Eruptive and environmental processes recorded by diatoms in volcanically dispersed lake sediments from the Taupo Volcanic Zone, New Zealand. *Journal of Paleolimnology* 54, 263–277. https:// doi.org/10.1007/s10933-015-9851-5

Jones J.T. & Segnit E.R. 1971: The nature of opal. Nomenclature and constituent phases. *Journal of the Geological Society of Australia* 18, 57–68.

Knox G. 1823: On bitumen in stones. *Philosophical Transactions of the Royal Society of London* 113, 517–528.

Kociolek J.P., Theriot E.C., Williams D.M., Julius M., Stoermer E.F. & Kingston J.C. 2015: Centric and Araphid Diatoms. In: Freshwater Algae of North America. *Academic Press*, 653–708. https://doi.org/10.1016/b978-0-12-385876-4.00015-3

Kotarba M.J. & Koltun Y.V. 2006: The origin and habitat of hydrocarbons of the Polish and Ukrainian parts of the Carpathian Province. In: Golonka J. & Pícha F. (Eds.): The Carpathians and Their Foreland: Geology and Hydrocarbon Resources. *AAPG Memoir* 84, 395–442. https://doi.org/10.1306/985605M843074

Kotlarczyk J. & Kaczmarska I. 1987: Two diatom horizons in the Oligocene and ?Lower Miocene of the Polish Outer Carpathians. *Annales Societatis Geolorum Poloniae* 57, 142–188.

Kováč M., Halásová E., Hudáčková N., Holcová K., Hyžný M., Jamrich M. & Ruman A. 2018: Towards better correlation of the Central Paratethys regional time scale with the standard geological time scale of the Miocene Epoch. *Geologica Carpathica* 69, 283–300. https://doi.org/10.1515/geoca-2018-0017

Krhovský J., Adamová J., Hladíková J. & Maslowská H. 1992: Paleoenvironmental changes across the Eocene/Oligocene boundary in the Ždánice and Pouzdřany units (Western Carpathians, Czechoslovakia): the long-term trend and orbitally forced changes in calcareous nannofossil assemblages. In: Nannoplankton research. *Proceedings of the 4th Nannoplankton Assoc. Conference*, 105–187.

Lafargue E., Marquis F. & Pillot D. 1998: Rock-Eval 6 Applications in Hydrocarbon Exploration, Production, and Soil Contamination Studies. *Oil and Gas Science and Technology* 53, 421–437.

Lampadius 1809: XXI. Analysis of the schist that accompanies the menilite near Paris. *The Philosophical Magazine* 33, 134–136.

Lohrenz S.E., Dagg M.J. & Whitledge T.E. 1990: Enhanced primary production at the plume/oceanic interface of the Mississippi River. *Continental Shelf Research* 10, 639–664. https://doi.org/10.1016/0278-4343(90)90043-l

Lueger O. 1904: Lexikon der gesamten Technik und ihrer Hilfswissenschaften. *Deutsche Verlags-Anstalt*, Stuttgart.

Melinte-Dobrinescu M. & Brustur T. 2008: Oligocene–Lower Miocene events in Romania. *Acta Palaeontologica Romaniae* 6, 203–215.

Mertz K.A. Jr. 1989: Origin of hemipelagic source rocks during early and middle Miocene, Monterey Formation, Salinas Basin, California. *AAPG Bulletin* 73, 510–524.

Moţaş I., Bandrabur T., Ghenea C. & Săndulescu M. 1968: Geological map L-35-XXVII, sheet 36 Ploieşti 1:200,000 [Harta geologică L-35-XXVII, foaia 36 Ploieşti la 1:200,000]. *Institutul Geologic al României*, Bucureşti (in Romanian).

Munteanu I., Popescu D., Borosi V., Dobre S., Maioru V. & Iusco G. 2014: Stratigraphic re-evaluation of the Oligocene-Lower Miocene formations in the Diapiric Fold Zone, Eastern Carpathian, Romania. In: European Regional Conference and Exhibition. Barcelona, Search and Discovery Article #90192.

Mutihac V. & Ionesi L. 1974: Geology of Romania. *Editura Tehnică,* Bucharest, 1–655.

Ognjanova-Rumenova N.G. & Crawford R.M. 2012: Morphology and ultrastructure of the fossil freshwater diatom *Aulacoseira temperei*. *Diatom research* 27, 107–119. https://doi.org/10.1080/0269249X.2012.696495

Ognjanova-Rumenova N.G. & Pipík R. 2015: Stratigraphic and taxonomic significance of siliceous microfossils collected from the Turiec Basin, Western Carpathians (Slovakia). *Acta Botanica Croatica* 74, 345–361. https://doi.org/10.1515/botcro-2015-0023

Ognjanova-Rumenova N.G. & Pipík R. 2018: *Aulacoseira turiecensis*, a new fossil species from the Turiec Neogene Basin, Slovakia. *Nova Hedwigia* Beihefte 147, 127–139.

Olshtynska A. 2001: Miocene marine biostratigraphy of the eastern Paratethys (Ukraine). *Geologica Carpathica* 52, 173–181.

Pantocsek J. 1886: Beiträge zur Kenntnis der Fossilen Bacillarien Ungarns. I. Theil: Marine Bacillarien. *Buchdrucherei von Julius Platzko*, Nagy-Tapolcsány, 1–76.

Pantocsek J. 1889: Beiträge zur Kenntnis der Fossilen Bacillarien Ungarns. Teil II. Brackwasser Bacillarien. Anhang: Analyse der marinen Depôts von Bory, Bremia, Nagy-Kürtös in Ungarn; Ananino und Kusnetzk in Russland. *Buchdrucherei von Julius Platzko*, Nagy-Tapolcsány, 1–123.

Paraschiv D. & Olteanu G. 1970: Oil fields in Mio-Pliocene zone of eastern Carpathians District of Ploiesti. *AAPG Bulletin* 52, 399–427. https://doi.org/10.1306/5d25c395-16c1-11d7-8645000102c1865d

Patrulius D., Ștefănescu M., Popa E. & Popescu I. 1968: Geology of the Inner Zones of the Carpathian Bend. *Geological Institute*, Romania, 1–50.

Pătruț I. 1955: Geology and tectonics of the Vălenii de Munte-Cosminele-Bustenari region [Geologia și tectonica regiunii Vălenii de Munte-Cosminele-Buștenari]. *Anuarul Comitetului Geologic* 28, 5–98 (in Romanian).

Pierer H.A. 1857: Pierer's Universal-Lexikon. Vol. 115, *Directmedia Publishing GmbH*.

Popescu B.M. 1995: Romania's petroleum systems and their remaining potential. *Petroleum Geoscience* 14, 337–350.

Popov S.V., Rögl F., Rozanov A.Y., Steininger F.F., Shcherba I.G. & Kováč M. (Eds.) 2004: Lithological–Paleogeographic maps of Paratethys. 10 Maps Late Eocene to Pliocene. *Courier Forschungsinstitut Senckenberg* 250, 1–46.

Radionova E. & Golovina L. 2011: Upper Maeotian–Lower Pontian "Transitional Strata" in the Taman Peninsula: stratigraphic position and paleogeographic interpretation. *Geologica Carpathica* 62, 77–90. https://doi.org/10.2478/v10096-011-0007-x

Rauball J.F., Sachsenhofer R.F., Bechtel A., Ćorić S. & Gratzer R. 2019: The Oligocene–Miocene Menilite Formation in the Ukrainian Carpathians: A world-class source rock. *Journal of Petroleum Geology* 42, 4, 393–416. https://doi.org/10.1111/jpg.12743

Řeháková Z. 1975: Marine diatoms in Helvetian sediments of the Central Paratethys. *Nova Hedwigia* 53, 293–303.

Řeháková Z. 1977: Marine planktonic diatom zones of the Central Paratethys Miocene and their correlation. *Věstník Ústředního ústavu geologického* 52, 147–157.

Rögl F. 1999: Mediterranean and Paratethys. Facts and hypotheses of an Oligocene to Miocene paleogeography short overview. *Geologica Carpathica* 50, 339–349.

Rothwell R.G. 1989: Minerals and mineraloids in marine sediments; an optical identification guide. *Elsevier Science Publishers*, 1–282. https://doi.org/10.1180/minmag.1991.055.379.23

Round F.E., Crawford R.M. & Mann D.G. 1990: Diatoms: biology and morphology of the genera. *Cambridge University Press*, 1–176.

Sachsenhofer R.F., Hentschke J., Bechtel A., Coric S., Gross D., Horsfield B., Rachetti A. & Soliman A. 2015: Hydrocarbon potential and depositional environments of Oligo-Miocene rocks in the Eastern Carpathians (Vrancea Nappe, Romania). *Marine and Petroleum Geology* 68, 269–290. https://doi.org/10.1016/j.marpetgeo.2015.08.034

Sachsenhofer R.F., Popov S.V., Bechtel A., Ćorić S., Francǔ J., Gratzer R., Grunert P., Kotarba M., Mayer J., Pupp M., Rupprecht B.J. & Vincent S.J. 2018a: Oligocene and Lower Miocene source rocks in the Paratethys: Palaeogeographic and stratigraphic controls. In: Simmons M.D., Tari G.C. & Okay A.I. (Eds.): Petroleum Geology of the Black Sea. *Geological Society Special Publication* 464, 267–306. https://doi.org/10.1144/SP464.1

Sachsenhofer R.F., Popov S.V., Ćorić S., Mayer J., Misch D., Morton M.T., Pupp M., Rauball J. & Tari G. 2018b: Parathethyan petroleum source rocks: an overview. *Journal of Petroleum Geology* 41, 3, 219–246. https://doi.org/10.1111/jpg.12702

Săndulescu M. 1984: Geotectonics of Romania [Geotectonica României]. *Editura Tehnica*, București, 1–280 (in Romanian).

Săndulescu M., Popescu G. & Mărunțeanu M. 1995: Facies and stratigraphy of the Lower and Middle Miocene formations of the Slănic Syncline. *Romanian Journal of Stratigraphy* 76, 3–11.

Săndulescu M., Stefănescu M., Butac A., Patrut I. & Zaharescu P. 1981: Genetical and structural relations between flysch and Molasse: The Eastern Carpathians Model. Guide to Excursion A5. *Institute of geology and geophysics,* Guide-book series 19, 1–94.

Schleder Z., Tămaș D.M., Krezsek C., Arnberger K. & Tulucan A. 2019: Salt tectonics in the Bend Zone segment of the Carpathian fold and thrust belt, Romania. *International Journal of Earth Sciences* 108, 1595–1614. https://doi.org/10.1007/s00531-019-01721-x

Schrader H. & Gersonde R. 1978: Diatoms and silicoflagellates. In: Zachariasse W.L. et al.: Microplaeontological counting methods and techniques, an excercise on an eight meters section of the lower Pliocene of Capo Rossello. Sicily. *Utrecht Micropaleontological Bulletins* 17, 129–176.

Schrader H.J. 1973: Proposal for a standardized method of cleaning diatoms-bearing deep-sea and land-exposed marine sediments. In Simonsen R. (Ed.): Seconds symposium on recent and fossil diatoms. *Nova Hedwigia* 45, 403–409.

Schultz L. 1964: Quantitative interpretation of mineralogical composition from X-ray and chemical data for the Pierre Shale. *U.S.G.S. Professional Paper* 391-C. https://doi.org/10.3133/pp391C

Schulz H.M., Bechtel A.C., Rainer T.H., Sachsenhofer R.F. & Struck U.L. 2004: Paleoceanography of the Western Central Paratethys during early Oligocene nannoplankton Zone NP23 in the Austrian Molasse Basin. *Geologica Carpathica* 55, 311–323.

Sebe-Rădoi O.G., Dumitras D.G., Marincea S., Calin N., Birgoanu D. & Barbu O.C. 2017: Preliminary paleontological and mineralogical study of the diatomites from Pătârlagele, Romania. *Goldschmidt Abstracts* 3579.

Simonsen R. 1979: The diatom system: ideas on phylogeny. *Bacillaria* 2, 9–71.

Ślączka A., Kruglov S., Golonka J., Oszczypko N. & Popadyuk I. 2006: Geology and hydrocarbon resources of the Outer Carpathians, Poland, Slovakia, and Ukraine: general geology. In: The Carpathians and their foreland: Geology and hydrocarbon resources. *AAPG Memoir* 84, 221–258. https://doi.org/10.1306/985610M843070

Smith D.K. 1998: Opal, cristobalite, and tridymite: noncrystallinity versus crystallinity, nomenclature of the silica minerals and bibliography. *Powder diffraction* 13, 2–19.

Smith S.A. & Hiscott R.N. 1987: Latest precambrian to Early Cambrian basin evolution, Fortune Bay, Newfoundland fault – bounded basin to platform. *Canadian Journal of Earth Sciences* 21, 1379–1392.

Smith W.O. & Demaster D.J. 1996: Phytoplankton biomass and productivity in the Amazon River plume: correlation with seasonal river discharge. *Continental Shelf Research* 16, 291–319. https://doi.org/10.1016/0278-4343(95)00007-n

Soták J. 2010: Paleoenvironmental changes across the Eocene–Oligocene boundary: insights from the Central-Carpathian Paleogene Basin. *Geologica Carpathica* 61, 393–418. https://doi.org/10.2478/v10096-010-0024-1

Ştefănescu M. 1978: Stratigraphy and structure of Cretaceous and Paleogene Flysch deposits between Prahova and Ialomiţa Valleys. *Faculty of Geology*, *University of Bucharest*, Bucharest 76, 1–47.

Ştefănescu M., Radan S., Micu M., Mărunţeanu M. & Ştefanescu M. 1978: Geological map of Slanic Prahova, scale 1:50,000 [Slanic Prahova Harta Geologică 129b, scara 1:50000]. *IGR,* Bucuresti (in Romanian).

Ştefănescu M., Dicea O. & Tari G. 2000: Influence of extension and compression on salt diapirism in its type area, East Carpathian Bend area, Romania. In: Vendeville B.C., Mart Y. & Vigneresse J.L. (Eds): Salt, shale and igneous diapirs in and around Europe. *Geological Society*, *London*, 174, 131–147. https://doi.org/10.1144/GSL. SP.1999.174.01.08

Ţabără D. 2010: Palynology, palynofacies and thermal maturation of the kerogen from the Moldavidian Domain Gura Humorului area. *Analele Ştiinţifice de Universităţii AI Cuza din Iaşi*, secţiunea 2, Geologie 56, 53.

Tămaş A., Tămaş D.M., Krezsek C., Schleder Z., Palladino G. & Bercea R. 2020: The nature and significance of sand intrusions in a hydrocarbon-rich fold and thrust belt: Eastern Carpathians Bend Zone, Romania. *Journal of the Geological Society* 177, 343–356. https://doi.org/10.1144/jgs2019-107

Tămaş D.M. 2018: Salt tectonics in the Eastern Carpathian Bend Zone, Romania. *PhD Thesis*, Babes-Bolyai University, Cluj-Napoca, 1–146.

Taylor J.C. 1976: Geological appraisal of the petroleum potential of offshore Southern California: The borderland compared to onshore coastal basins. *US Department of the Interior. Geological Survey Circular* 730, 43.

Triplehorn D.M. 1965: Origin and significance of glauconite in the geologic sequence. *Tulsa Geological Society Digest* 33, 282–283.

Usoltseva M., Khursevish G., Rasskazov S., Vorob'eva S. & Chernyaeva G. 2010: Morphology of *Actinocyclus* and *Lobodiscus* species (Bacillariophyta) from the Miocene deposits of the Vitim Plateau, Russia. *Plant Ecology and Evolution* 143, 352–364. https://doi.org/10.5091/plecevo.2010.410

Vasiliu V.E., Frunzescu D. & Cehlarov A. 1996: Mineralogical, petrographic and geochemical study of diatomites from the Sibiciu de Sus, Pătârlagele [Studiul mineralogic, petrografic şi geochimic al diatomitelor de la Sibiciu Pătârlagele]. *Revista Română de Petrol* 3, 62–66 (in Romanian).

Wendorff M., Rospondek M., Kluska B. & Marynowski L. 2017: Organic matter maturity and hydrocarbon potential of the Lower Oligocene Menilite facies in the Eastern Flysch Carpathians (Tarcău and Vrancea Nappes), Romania. *Applied Geochemistry* 78, 295–310. https://doi.org/10.1016/j.apgeochem.2017.01.009

Zolitschka B. 1998: Paläoklimatische Bedeutung laminierter Sedimente. Holzmaar Eifel, Deutschland, Lake C2 Nordwest-Territorien, Kanada und Lago Grande di Monticchio Basilicata, Italien. *Bornträger*, Berlin, 1–176.